A gene-fusion strategy for stoichiometric and co-localized expression of light-gated membrane proteins

Sonja Kleinlogel[1], Ulrich Terpitz[1,4], Barbara Legrum[1], Deniz Gökbuget[1,4], Edward S Boyden[2], Christian Bamann[1], Phillip G Wood[1] & Ernst Bamberg[1,3]

The precise co-localization and stoichiometric expression of two different light-gated membrane proteins can vastly improve the physiological usefulness of optogenetics for the modulation of cell excitability with light. Here we present a gene-fusion strategy for the stable 1:1 expression of any two microbial rhodopsins in a single polypeptide chain. By joining the excitatory channelrhodopsin-2 with the inhibitory ion pumps halorhodopsin or bacteriorhodopsin, we demonstrate light-regulated quantitative bi-directional control of the membrane potential in HEK293 cells and neurons *in vitro*. We also present synergistic rhodopsin combinations of channelrhodopsin-2 with *Volvox carteri* channelrhodopsin-1 or slow channelrhodopsin-2 mutants, to achieve enhanced spectral or kinetic properties, respectively. Finally, we demonstrate the utility of our fusion strategy to determine ion-turnovers of as yet uncharacterized rhodopsins, exemplified for archaerhodopsin and CatCh, or to correct pump cycles, exemplified for halorhodopsin.

Most genetic engineering technologies focus on the strong expression of a single gene, but the accurate control of cell physiology often requires precise control of expression of multiple proteins. The popular optogenetic approach to control neuronal excitability is based on the expression of the light-activated microbial rhodopsins channelrhodospin-2 (ChR2)[1] from *Chlamydomonas reinhardtii,* a cation-permeable channel that enables cell depolarization (neuronal activation) in response to blue light, and halorhodopsin from *Natromonas pharaonis* (NphR or Halo)[2,3], a chloride pump that enables cell hyperpolarization (neuronal silencing) in response to orange light. A major technical challenge in optogenetics is to express ChR2 and NphR together in defined ratios in a cell so that neuronal activation and silencing can be precisely controlled.

Equal-copy-number and co-localized expression of the two proteins would be beneficial for studies of sufficiency and necessity of a given class of neurons for a behavior or a pathology in the same animal doing a given task or, alternatively, allow to survey how neuronal computations occur in the intact brain by altering the timing of neuronal activity without altering the basal firing rate of neurons[2,4]. The ability to drive and block electrical activity at defined locations, for example, at a dendritic spine or a synaptic terminal, would also be beneficial and again requires co-localization of ChR2 and NphR.

From a functional aspect, ratiometric expression of two rhodopsins in a cell represents a new strategy to determine the relative ion-transport activity of one protein against the other. Particularly, it enables direct comparison of specific activities of new channelrhodopsin and inhibitory pump variants to those of standard ChR2 and NphR, while excluding effects owing to differences in expression or membrane localization. Finally, this calibration method is presumably extendable to other monomeric membrane proteins and could allow a direct determination of expression and specific activities relative to those of rhodopsins with known transport properties.

Previous approaches for the co-expression of two light-activated proteins with approximately equal copy number under a single promoter have included the use of internal ribosomal entry sites (IRESs)[4] or self-cleaving viral peptide bridges, namely 2A or 2A-like peptide sequences[5–8]. The 2A peptides have led to more equal protein expression compared to the traditional strategy of using IRESs, but nevertheless, the 2A peptide–cleaved ChR2 and NphR can be shuttled to different membrane locations and their different degradation rates can lead to variable stoichiometries of expression. To overcome these limitations, we present a genetic tandem cassette that allows stoichiometric and co-localized expression of two rhodopsins in a single fusion protein. We combined the genes encoding two light-gated microbial rhodopsins via the coding sequences of a fluorescent protein (enhanced YFP (EYFP) or monomeric (m)Kate) and an additional transmembrane helix from the β subunit of the rat gastric H^+,K^+-ATPase for expression of a single fusion protein. We obtained evidence for the expression of functional tandem proteins by western blot analysis and electrophysiological characterization.

[1]Max Planck Institute of Biophysics, Department of Biophysical Chemistry, Frankfurt am Main, Germany. [2]The Massachusetts Institute of Technology Media Laboratory, Synthetic Neurobiology Group and Department of Biological Engineering, Massachusetts Institute of Technology, Cambridge, Massachusetts, USA. [3]Chemical and Pharmaceutical Sciences Department, Johann Wolfgang Goethe University Frankfurt, Frankfurt am Main, Germany. [4]Present addresses: Department of Biotechnology and Biophysics, Julius Maximilians University Würzburg, Biocenter Am Hubland, Würzburg, Germany (U.T.) and Eidgenössische Technische Hochschule Zürich, Institute of Cell Biology, Zurich, Switzerland (D.G.). Correspondence should be addressed to E.B. (ernst.bamberg@mpibp-frankfurt.mpg.de).

RECEIVED 7 APRIL; ACCEPTED 19 SEPTEMBER; PUBLISHED ONLINE 6 NOVEMBER 2011; DOI:10.1038/NMETH.1766

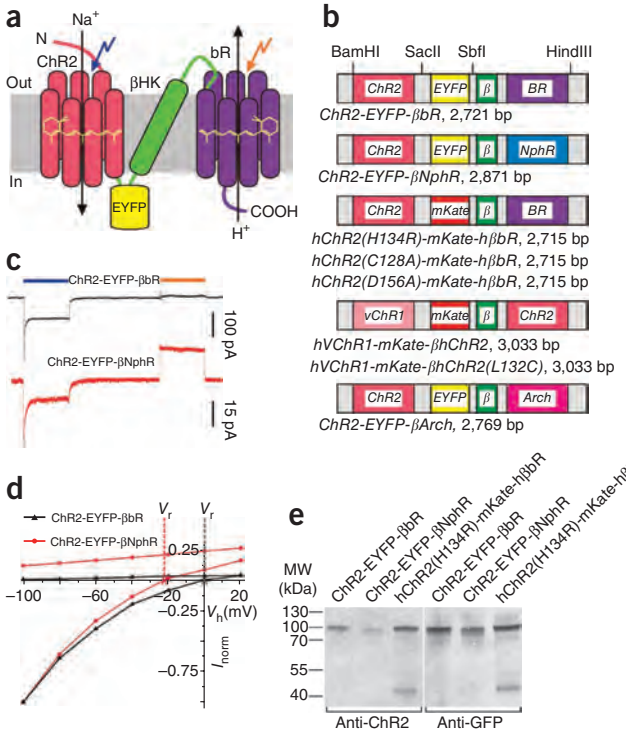

Figure 1 | Design of protein chimeras and functional evaluation of ChR2-EYFP-βbR, ChR2-EYFP-βNphR and hChR2(H134R)-mKate-hβbR. (**a**) Schematic drawing of the ChR2-EYFP-βbR construct after ligation of ChR2-EYFP with βbR. βHK, β helix derived from the H^+,K^+-ATPase β subunit; bR, bacteriorhodopsin. Blue and orange arrows indicate light spectrum that preferentially activates each protein. (**b**) Diagrams of the tandem expression cassette variants presented in this paper. *h* indicates human codon-optimized sequence; bp, base pairs. (**c**) Typical photocurrents measured at −40 mV in ChR2-EYFP-βbR– and ChR2-EYFP-βNphR–expressing HEK293 cells evoked by sequential equiphoton blue and orange 1-s illumination (bars). (**d**) Representative current-to-voltage relationships of ChR2 (inward rectifying) and bacteriorhodopsin or NphR (linear) in ChR2-EYFP-βbR and ChR2-EYFP-βNphR, normalized to the ChR2 current at −100 mV. V_r, reversal potential; V_h, membrane holding potential; *I*, current. (**e**) Western blot analyses of transiently transfected HEK293 cells. Cell lysates comprising 30 µg of protein were analyzed with a monoclonal ChR2 antibody (anti-ChR2) and with an antibody to GFP (anti-GFP). The 100-kDa bands represent the full-length fusion proteins, the 40-kDa band of hChR2(H134R)-mKate-hβbR represents an additional proteolytic fragment.

RESULTS

Design of the tandem expression cassette

It is impossible to directly connect ChR2 and NphR in a functional fusion protein, as the C terminus of ChR2 is on the intracellular side of the cell membrane whereas the N terminus of NphR is on the extracellular side. In an initial attempt to fuse the two proteins, we replaced NphR by a variant of the inhibitory proton pump bacteriorhodopsin from *Halobacterium salinarum* that contains an additional N-terminal transmembrane β helix (βbR) so that its N terminus is located intracellularly[9]. This β helix is the 105-amino-acid N-terminal fragment of the β subunit of the rat gastric H^+,K^+-ATPase, which supports membrane trafficking of bacteriorhodopsin and leads to an approximately tenfold increase in expression[9]. Whereas a fusion of only ChR2(1–309) with βbR was a nonfunctional protein (data not shown), a fusion of ChR2(1–309)–EYFP with βbR resulted in functional expression (ChR2-EYFP-βbR, **Fig. 1a**,**b**). We used the same expression cassette to combine ChR2 with NphR via the EYFP–β linker (ChR2-EYFP-βNphR, **Fig. 1b**). Analogous to bacteriorhodopsin, the addition of the β loop to NphR similarly improved expression (data not shown).

Bidirectional tandem proteins expressed in HEK293 cells

We examined functionalities of ChR2-EYFP-βbR and ChR2-EYFP-βNphR in transiently transfected HEK293 cells. We activated ChR2 and NphR or bacteriorhodopsin by 473-nm (blue) and 593-nm (orange) light of saturating photon densities, respectively. In voltage-clamp experiments, EYFP-expressing HEK293 cells showed rapid inward ChR2 currents upon 473-nm illumination and NphR or bacteriorhodopsin outward pump currents upon 593-nm illumination (**Fig. 1c**). Whereas ChR2 yielded an inwardly rectifying current-voltage relationship, the current-voltage behaviors of both NphR[3,10] and bacteriorhodopsin[11] were linear and strictly outward directed (**Fig. 1d**). The relative NphR current was markedly increased compared to the ChR2 current in ChR2-EYFP-βNphR in comparison to the bacteriorhodopsin current in ChR2-EYFP-βbR (**Fig. 1c**). As a consequence, the ChR2 reversal potential was shifted by approximately −20 mV (**Fig. 1d**) owing to co-activation of NphR and ChR2 during 473-nm illumination (**Supplementary Fig. 1**) and the summation of currents of opposite signs. The amount of the negative shift of the ChR2 reversal potential depends on the chosen ChR2-activation wavelength, which may co-activate NphR to a greater or lesser extent. ChR2 was not activated by 593-nm light (**Supplementary Fig. 1**) and the observed currents under orange illumination were pump currents only. Similarly, the stronger specific activity of NphR compared to that of bacteriorhodopsin was responsible for the smaller ChR2-induced depolarization in ChR2-EYFP-βNphR (7.9 ± 0.4 mV, −40 mV, mean ± s.e.m., $n = 5$) compared to ChR2-EYFP-βbR (18.5 ± 3.1 mV, −40 mV, mean ± s.e.m., $n = 5$).

As HEK293 cells expressed approximately threefold more ChR2-βbR copies than ChR2-EYFP-βNphR copies (**Table 1**), we focused on ChR2-EYFP-βbR for additional modifications. To avoid spectral overlap of the fluorescent marker with the channelrhodopsin absorption spectrum and to assess whether the globular spacer protein is exchangeable without loss of function, we replaced EYFP by the far-red fluorescent protein mKate[12]. To increase current amplitudes we (i) introduced the point mutation H134R into ChR2, which increases ChR2 activity by approximately 1.3-fold[1,13] (**Table 1**) and (ii) synthesized ChR2(H134R) and bacteriorhodopsin sequences optimized for human codon usage, hChR2(H134R) and hβbR, respectively. These modifications increased protein expression, current amplitudes (**Table 1**) and membrane potential shifts (hChR2(H134R), 42.4 ± 3.3 mV, $n = 5$, hβbR: −24.0 ± 5 mV, $n = 5$; −40 mV, mean ± s.e.m.) compared to ChR2-EYFP-βbR (**Table 1**).

Low cell-to-cell variability of the excitation-to-inhibition ratios (**Table 1**) across ChR2-EYFP-βNphR–, ChR2-EYFP-βbR– and hChR2(H134R)-mKate-hβbR–expressing HEK293 cells supports the exclusive existence of full-length transcripts and excludes post-translational tandem protein cleavage, which would lead to unequal expression of active pump and ChR2 copies. Western blot analyses from HEK293 cell lysates with a monoclonal antibody to ChR2 that specifically detects the C terminus of ChR2(1–309) (**Supplementary Fig. 2** and **Supplementary Note 1**) and with antibody to GFP revealed bands at ~100 kDa, confirming full-length fusion protein expression (**Fig. 1e**). Blots of hChR2(H134R)-mKate-hβbR revealed an additional 40-kDa proteolytic fragment,

Table 1 | Overview of rhodopsin-tandem properties versus single rhodopsins expressed in cultured HEK293 and hippocampal cells

Construct	$I(ChR2)_{stat}$ (pA/pF) −60 mV, 473 nm[a]	$I(pump)_{stat}$ (pA/pF) 0 mV, 593 nm[a]	$I(ChR2)_{stat}$: $I(pump)_{stat}$ ratio (mean ± s.e.m.)	Expression (copies μm^{-2})[b]	Relative pump activity[c]	Calculated pump turnover[b]	Pump current relaxation[d]	τ_{off} channel (ms; mean ± s.e.m.)	n[e]
ChR2-EYFP-βbR	−15.1 ± 2.1 −2.28 ± 0[f]	0.7 ± 0.2 0.10 ± 0.04[f]	19.5 ± 0.9 21.1 ± 1.6[f]	339	1	140 s^{-1}	169 s^{-1} (82%) 8.2 s^{-1} (18%)	–	5
ChR2-EYFP-βNphR	−4.4 ± 0.3 −0.25 ± 0.09[f]	1.7 ± 0.1 0.1 ± 0.03[f]	2.6 ± 0.1 2.5 ± 0.1[f]	99	8	1,245 s^{-1}	533 s^{-1}	–	5
hChR2(H134R)-mKate-hβbR	−32.1 ± 9.4 −4.65 ± 0.77[f]	1.6 ± 0.3 0.22 ± 0.06[f]	21.0 ± 0.2 20.3 ± 0.9[f]	445	1	197 s^{-1}	175 s^{-1} (78%) 16 s^{-1} (22%)	–	5
ChR2-EYFP-βArch	−17.1 ± 2.8	5.0 ± 2.8	3.9 ± 0.7	386	6	821 s^{-1}	535 s^{-1} (81%) 50 s^{-1} (19%)	–	7
hChR2(D156A)-mKate-hβbR	−9.0 ± 3.5	0.6 ± 0.1	10.1 ± 1.2	202	–	–	–	134 ± 3[g]	5
hVChR1-mKate-βhChR2	−12.16 ± 2.5 −3.45 ± 0.26[f]	–	–	–	–	–	–	17 ± 1 (1)[h] 107 ± 5 (2)[h]	6
hVChR1-mKate-βhChR2(L132C)	−14.3 ± 2.4	–	–	–	–	–	–	28 ± 3 (1)[h] 108 ± 7 (2)[h]	5
βbR	–	0.9 ± 0.5	–	419	–	–	157 s^{-1} (86%) 7.8 s^{-1} (14%)	–	3
hβNphR	–	1.8 ± 0.1	–	103	–	–	517 s^{-1}	–	3
Arch	–	6.4 ± 0.3	–	417	–	–	534 s^{-1} (72%) 48 s^{-1} (28%)	–	3
ChR2	10.1 ± 1.7 (ref. 22)	–	–	227	–	–	–	10 ± 1 (ref. 13)	6
hChR2	16.0 ± 1.5	–	–	360	–	–	–	10 ± 1	5
ChR2(H134R)	20.3 ± 7.2	–	–	281	–	–	–	19 ± 3 (ref. 13)	5
hVChR1	10.6 ± 3.0	–	–	–	–	–	–	95 ± 8	5
ChR2(L132C)	25.0 ± 8.8 (ref. 22)	–	–	–	–	–	–	16 ± 3 (ref. 23)	5

All constructs were expressed transiently and measured under identical conditions.
[a]Steady-state current densities at saturating light intensities (mean ± s.e.m.). [b]Calculated from ChR2 current densities under consideration of the ChR2 desensitization. [c]Calculated from $I(ChR2)_{stat}$: $I(pump)_{stat}$ ratios relative to ChR2-EYFP-βbR. [d]Rate constants from current relaxation at end of 593 nm illumination ($k_{off}(1)$, $k_{off}(2)$). The relative amplitudes are given in parentheses in case of a biexponential decay. [e]Recorded cells. [f]Current densities in cultured hippocampal neurons (all others were recorded in HEK293 cells). [g]Measured under 593-nm illumination. All other values are determined in the dark at the end of 473-nm illumination. [h]Biphasic τ_{off} from VChR1 (1) and ChR2 or ChR2(L132C) (2).

which had no influence on the 1:1 stoichiometry of functional pumps and channels (**Fig. 1e** and **Table 1**).

Validation of bidirectional tandem activity in neurons

We transduced cultured rat hippocampal neurons with recombinant adeno-associated viruses (rAAV) carrying sequences encoding ChR2-EYFP-βbR, ChR2-EYFP-βNphR and hChR2(H134R)-mKate-hβbR under a short *HIV-LTR* sequence with promoter activity[14]. All constructs were expressed homogenously throughout the cell membrane, including axons and dendrites (**Fig. 2a**). Voltage-clamp recordings showed that exposure to orange or blue light led to outward or inward photocurrents, respectively (**Fig. 2b** and **Table 1**). In current-clamp experiments, blue light reliably induced a train of action potentials, and orange light hyperpolarized the membrane potential (**Fig. 2c**). As in transiently transfected HEK293 cells, hChR2(H134R)-mKate-hβbR was the most potent bi-directional switch, inducing depolarization and hyperpolarization membrane potential shifts of twice the amplitudes (19.4 ± 2.8 mV; −11.0 ± 1.9 mV, $n = 4$, mean ± s.e.m.) of ChR2-EYFP-βbR (8.9 ± 1.6 mV; −5.7 ± 1.4 mV; $n = 5$, mean ± s.e.m.) and approximately fourfold the amplitudes of ChR2-EYFP-βNphR (4.2 ± 1.3 mV; −5.9 ± 1.1 mV; $n = 4$, mean ± s.e.m.). Sustained 473-nm illumination drove reliable spike trains, which could be temporarily silenced by concomitant 593-nm illumination (**Fig. 2d** and **Supplementary Fig. 3a**). To achieve optimal silencing with blue-orange double illumination, we had to reduce the 473-nm intensity relative to the 593-nm intensity (10^{19} photons s^{-1} cm^{-2}) by a factor of ~30 in ChR2-EYFP-βbR–expressing cells owing to the larger ChR2 currents (**Supplementary Fig. 3b**,**c**). We confirmed temporal precision of photostimulation by the observation of single-spike induction with 10-ms blue laser pulses, which were suppressed by concomitant orange light (**Fig. 2e**). Thus, the tandem proteins (ChR2-EYFP-βbR, ChR2-EYFP-βNphR and hChR2(H134R)-mKate-hβbR) showed the expected action on hippocampal cells reflecting the proper function of the two rhodopsins.

Synergistic rhodopsin combinations

Synergistic combinations of light-gated rhodopsins can create more powerful optogenetic tools. The slowly cycling mutants[15,16] hChR2(C128A) and hChR2(D156A) are activated by a brief pulse of blue light and remain open for minutes if not closed prematurely by orange light illumination. Nevertheless, orange light off-switching still remains slow relative to the wild-type ChR2 (hundreds of milliseconds versus 5–10 ms). The combination of these slow mutants with hβbR in tandem (**Fig. 1b**) enabled us to accelerate the apparent orange light off-switching time (τ_{off}) by at least twofold in HEK293 cells, from an initial τ_{off} of 250 ± 10 ms for hChR2(C128A) to 140 ± 3.5 ms in hChR2(C128A)-mKate-hβbR (mean ± s.e.m., $n = 4$; **Supplementary Fig. 4a**) and from 483 ± 11 ms for hChR2(D156A) to 134 ± 2.5 ms in hChR2(D156A)-mKate-hβbR (mean ± s.e.m., $n = 4$; **Fig. 3a**). Orange light did not only activate proton pumping by hβbR but also led to an accelerated closing of the channel in ChR2(C128A) or ChR2(D156A)[15,16] owing to the presence of a red-shifted photointermediate in the open state (P520, maximum absorbance at 520 nm) that can undergo photoreaction back into the blue-excitable ground

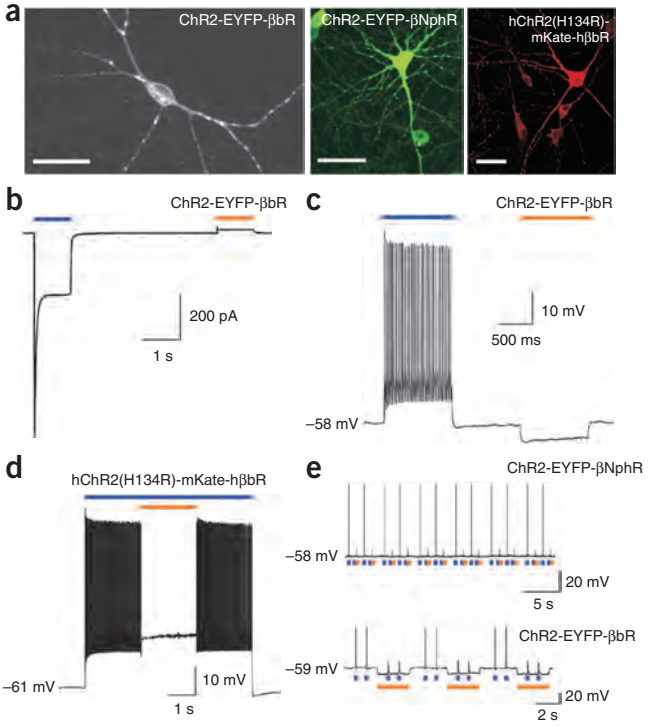

Figure 2 | Expression and functionality of bidirectional rhodopsin tandem proteins in cultured hippocampal neurons. (**a**) Apotome (left) and confocal (middle and right) images of hippocampal neurons expressing ChR2-EYFP-βbR, ChR2-EYFP-βNphR or hChR2(H134R)-mKate-hβbR. Scale bars, 50 µm. (**b**) Representative voltage-clamp recording of neurons expressing ChR2-EYFP-βbR exposed to 473-nm (blue bar) and 593-nm (orange bar) light (–60 mV, $J_{473/593}$ 1.4 × 10^{19} photons s^{-1} cm^{-2}). (**c**) Representative current-clamp recording of hippocampal neurons expressing ChR2-EYFP-βbR exposed to 473-nm (blue bar) and 593-nm (orange bar) light ($J_{473/593}$ 1.4 × 10^{19} photons s^{-1} cm^{-2}). (**d**) Representative current-clamp recording of neurons simultaneously exposed to 473-nm (6.4 × 10^{17} photons s^{-1} cm^{-2}) and 593-nm light (1.1 × 10^{19} photons $s^{-1}cm^{-2}$). (**e**) Representative current-clamp recordings of neurons exposed to 10-ms blue light pulses (J_{473} 2.25 × 10^{18} photons s^{-1} cm^{-2}) and simultaneous 593-nm light pulses (top; J_{593} 2.25 × 10^{18} photons s^{-1} cm^{-2}) or 593-nm background illumination (bottom; J_{593} 1.6 × 10^{19} photons s^{-1} cm^{-2}). Bars indicate periods of illumination.

state (absorbance maximum at 450 nm). Both effects counteracted the blue light–induced currents in hChR2(C128A) and hChR2(D156A) and led to accelerated off-switching of channelrhodopsin currents in the tandem chimeras (**Supplementary Fig. 4b**). In addition, the initial fast and oppositely directed bacteriorhodopsin current with a τ_{on} of only 70 µs (**Supplementary Note 2**) reduced the net current amplitude to ~66% (**Fig. 3a** and **Supplementary Fig. 4b**), which may suffice to silence neurons on a sub-millisecond regime near the activation threshold.

We also combined the blue light–activated hChR2 with the green light–activated *V. carteri* channelrhodopsin-1 (hVChR1; ref. 17) to construct a wavelength-independent variant for neuronal stimulation (hVChR1-mKate-βhChR2) (**Fig. 1b**, **Supplementary Fig. 5** and **Supplementary Note 3**). We transiently transfected neuroblastoma cells with constructs encoding hVChR1-mKate-βhChR2, hVChR1 or hChR2 and illuminated the cells with short 1-ms light pulses of different wavelengths. We determined the action spectrum of hVChR1-mKate-βhChR2 and compared it to the action spectra of hVChR1 or hChR2. The broad hVChR1-mKate-βhChR2 spectrum consists of the sum of the hVChR1 and hChR2 spectra and covers the visible range, 400–650 nm (**Fig. 3b**). In rAAV-transduced hVChR1-mKate-βhChR2–expressing hippocampal neurons, 532-nm light of half-intensity induced similar current amplitudes (–3.27 ± 0.28 pA/pF; mean ± s.e.m., –60 mV, n = 5) as full-intensity illumination with 473-nm (–3.45 ± 0.26 pA/pF; mean ± s.e.m., –60 mV, n = 5) and 593-nm light (–2.52 ± 0.25 pA/pF; mean ± s.e.m., –60 mV, n = 5), respectively, reflecting an absorption overlap of hChR2 and hVChR1 in the green range of the spectrum (**Fig. 3c**). All three wavelengths induced reliable spikes in pyramidal neurons by depolarizing the membrane potential by ~20 mV (473 nm: 19.6 ± 1.6 mV, 532 nm: 19.9 ± 1.7 mV, 593 nm: 18.8 ± 1.9 mV; n = 5, mean ± s.e.m.; **Fig. 3c**) confirming the broad activation spectrum of hVChR1-mKate-βhChR2 and its suitability for neuronal broadband stimulation.

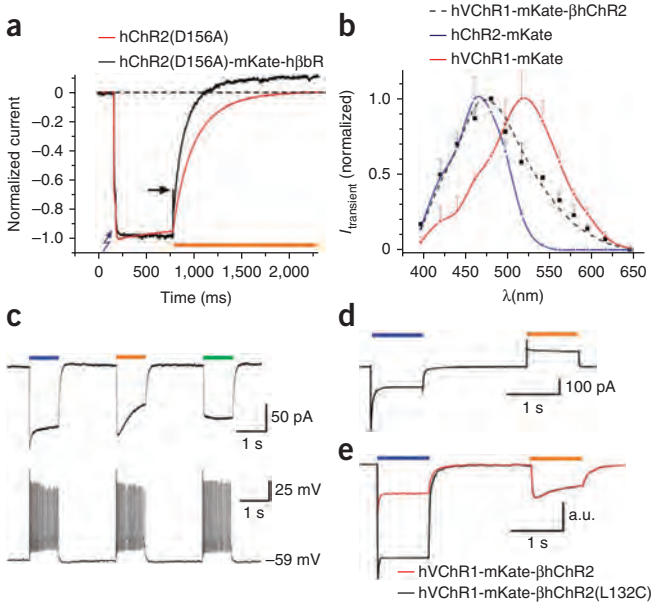

Figure 3 | Properties of rhodopsin tandem variants measured in HEK293 cells and hippocampal neurons. (**a**) Orange-light–induced off-switching of hChR2(D156A) and hChR2(D156A)-mKate-hβbR expressed in transiently transfected HEK293 cells and activated with a 5-ms blue light pulse (blue). Measurements were conducted at –60 mV; orange light onset is indicated by a black arrow. (**b**) Action spectra of hVChR1-mKate (n = 5), hChR2-mKate (n = 5) and hVChR1-mKate-βhChR2 (n = 5) determined in HEK293 cells based on 1-ms light pulses (2.5 × 10^{17} photons s^{-1} cm^{-2}, –60 mV). The black dashed curve was calculated from $I = I_{ChR2} + 1.7 \times I_{hVChR1}$. (**c**) hVChR1-mKate-βhChR2 expressed in hippocampal pyramidal cells. Typical photocurrents evoked by 1-s 473-nm (blue bar), 593-nm (orange bar) and 532-nm (green bar) light pulses in hippocampal pyramidal cells expressing hVChR1-mKate-βhChR2. Representative whole-cell current-clamp recording (bottom, $J_{473/593}$ 2.2 × 10^{19} photons s^{-1} cm^{-2}, J_{532} 1.2 × 10^{19} photons s^{-1} cm^{-2}). (**d**) Typical ChR2-EYFP-βArch photocurrents ($J_{473/593}$ 7.6 × 10^{18} photons s^{-1} cm^{-2}) measured at –40 mV in HEK293 cells. (**e**) Overlay of representative responses of hVChR1-mKate-βhChR2 and hVChR1-mKate-βhChR2(L132C) to 1-s pulses of 473-nm (blue bar) and 593-nm (orange bar) light (1.7 × 10^{19} photons s^{-1} cm^{-2}). Currents were normalized to the respective hVChR1 responses.

Determination of ion-turnover numbers

In light-driven ion pumps, such as bacteriorhodopsin or NphR, a single ion is translocated per photocycle that is triggered by light-induced retinal isomerization and characterized by a sequence of photointermediates responsible for ion uptake, transfer, release and chromophore recycling. In contrast to ChR2, for which many ions are conducted during the photocycle, the pump ion-transport rates are limited by the photocycle time that is needed to return to the ground state. In tandem expressing cells, transport rates can be calculated from the ChR2-to-pump current ratios (**Table 1**) and the known ChR2 single-channel conductance[13] (Online Methods). The calculated NphR ion turnover in ChR2-EYFP-βNphR was approximately ninefold greater than that of bacteriorhodopsin in ChR2-EYFP-βbR (**Table 1**). This contradicts spectroscopic data in which the NphR photocycle (~20–50 s^{-1})[18,19] is by at least a factor of two slower than that of bacteriorhodopsin (~100 s^{-1})[20]. In NphR, chloride release and uptake are monitored by the so-called L and O states of the photocycle, which decay within 1.5 ms into a state NphR′ resembling the ground state NphR[18]. The final slow transition from NphR′ to NphR with a time constant of 20 ms was assumed to be the rate-limiting step. However, under stationary light conditions, this slow step is irrelevant to the NphR turnover because the last two spectroscopically indistinguishable states NphR′ and NphR are both excitable by orange light[18] leading to an apparent acceleration of the photocycle time. Rate-limiting is therefore only the formation of NphR′, which takes 1.5 ms and is equivalent to τ_{off} (**Supplementary Note 2**).

Tandem chimeras can be used to discriminate whether an observed macroscopic current increase of a new rhodopsin variant is solely due to elevated expression or an actual increase of the ion-translocation rate per molecule. This is exemplified by the new inhibitory microbial proton pump archaerhodopsin-3 (Arch) from *Halorubrum sodomense*[21] and the recently described ChR2(L132C) point mutant CatCh[22].

Arch exhibits approximately sixfold increased pump currents compared to bacteriorhodopsin when expressed in cultured hippocampal neurons[21] and HEK293 cells (**Fig. 3d** and **Supplementary Fig. 6**). This observed current increase is due to an actual sixfold accelerated Arch ion turnover compared to that of bacteriorhodopsin as calculated from the currents measured for ChR2-EYFP-βArch (**Fig. 1b** and **Table 1**). Arch's high proton pump rate with the potential to induce strong cell hyperpolarizations without causing large pH swings[22] renders Arch an equally potent neuronal silencer as the commonly used expression-enhanced NphR (eNphR 3.0)[8] (**Supplementary Note 2** and **Supplementary Fig. 6**).

When expressed in HEK293 cells, CatCh mediates currents three times larger than those of wild-type ChR2 (ref. 22). The approximately 1.5-fold increase in CatCh's open-channel lifetime (**Table 1**) can only partially account for the observed photocurrent increase, and CatCh's unit conductance is not changed substantially compared to that of wild-type ChR2 (refs. 13,22). We used the tandem operator hVChR1-mKate-βhChR2(L132C) (**Fig. 1b**) to compare CatCh's current amplitude relative to that of ChR2. The normalized CatCh steady-state current in hVChR1-mKate-βhChR2(L132C) is approximately three times larger than the normalized ChR2 steady-state current in hVChR1-mKate-βhChR2 (**Fig. 3e**), leading to the conclusion that CatCh's increased current amplitudes are not due to increased protein expression but to a combination of a reduced desensitization[22] and slightly increased unit conductance and/or open probability compared to wild-type ChR2.

DISCUSSION

The genetic cassette we described can, in principle, be used for any two rhodopsins (as long as the absorption spectra are separated) and perhaps other monomeric membrane proteins. The EYFP or mKate intervening sequence serves as a spacer in the tandem sandwich, and possibly it could be substituted by other GFP variants or non-fluorescent[23,24] soluble proteins as long as sufficient freedom and flexibility is provided between the first protein and the β helix connected to the second protein.

Clear advantages of the tandem expression system compared to the IRES–based[4] or 2A-peptide–based[5–8] approaches are the guarantee for co-localization and strict ratiometric expression of the two proteins. Exact 1:1 protein ratios are the key for the use of tandem proteins for direct comparison of rhodopsin activities in which one of the rhodopsins is used as internal reference, for example, ChR2. With an increasing choice of rhodopsin variants such direct activity comparison allows the user to differentiate between an actual increase of the specific activity of the new variant and a current increase simply owing to overexpression. Taking into account the ChR2 single-channel conductance and its desensitization[25], which reduces the number of active ChR2 molecules to one third (data not shown), we determined the absolute turnover numbers of membrane channels and pumps using the rhodopsin tandem proteins. The values we obtained were subject only to a possible systematic error stemming from the small ChR2 single-channel conductance value[13] (Online Methods). The calculated pump ion turnover of bacteriorhodopsin, which we regard as a benchmark for our strategy, agrees well with published data once small variations owing to cell type (oocytes ~30 s^{-1})[9], conditions (purple membranes ~100 s^{-1})[19] and possibly subtle conformational changes owing to the ChR2 linkage are taken into account.

Using our model, we obtained an accelerated ion-turnover value for NphR compared to spectroscopically determined values[18,19]. This is explained by an orange light–induced photoreaction of the late intermediate NphR′, which accelerates the photocycle under stationary light conditions. This is in accordance with Fourier transform infrared spectrometry data revealing re-isomerization of the chromophore to the all-*trans* state in NphR′ and in the ground state NphR[26], a prerequisite to restart the photocycle and chloride transport. Furthermore, the proton pumps bacteriorhodopsin and Arch have two decay time constants indicative of the population of an inactive state (M*) in a nontransporting photocycle[9]. Usually, proton transfer is linked to the de- and reprotonation of the Schiff base corresponding to the respective formation and decay of a photointermediate known as the M state. By contrast, the inactive M* state is the result of a branching reaction where protons are not transported across the cell membrane. The presence of the M* state in bacteriorhodopsin and Arch may reduce their pump efficiencies compared to the chloride pump NphR with a monoexponential decay time and no loss of active pump molecules upon deprotonation of the Schiff base[27] (**Supplementary Note 2**). As a result, the NphR activity is increased compared to Arch despite comparable relaxation rates for the main electrogenic steps (**Table 1**).

For neuroscientists, the tandem-protein–based approach opens the way new kinds of experiments. For example, tethering of excitatory channelrhodopsins with inhibitory ion pumps for stoichiometric expression in the same neuron enables disruption of the precise spike timing[2] in a controlled manner. The tandem is superior to normal co-expression as the 473-nm-to-593-nm intensity ratio for optimized current cancellation (**Supplementary Fig. 3b**,**c**) remains constant across cells and only depends on the chosen channelrhodopsin-pump combination and the spectral overlap of the two proteins (**Supplementary Fig. 1**). All the neurons in a field of view can be activated or silenced to a similar extent by insertion or deletion of identical numbers of spikes from a train of action potentials. Furthermore, each patch of membrane will preserve the stoichiometry, enabling local control of cellular functions such as simulation of precise subthreshold events on synaptic spines or synaptic terminals.

METHODS

Methods and any associated references are available in the online version of the paper at http://www.nature.com/naturemethods/.

Accession codes. Genbank: JN836740, JN836741, JN836742, JN836743, JN836744, JN836745, JN836746 and JN836747.

Note: Supplementary information is available on the Nature Methods website.

ACKNOWLEDGMENTS

We thank V. Busskamp and B. Roska (Friedrich Miescher Institute for Biomedical Research, Basel) for the pAAV-LTR-EGFP plasmid and help with the rAAV construction, I. Bartnik for preparation of hippocampal neuron cultures, and H. Biehl and V. Eulenburg (Max Planck Institute for Brain Research, Frankfurt) for help with the antibody screening. The transgenic mouse expressing ChR2-EYFP was a gift from H. Wässle (Max Planck Institute for Brain Research, Frankfurt). The pAAV2-Rho-EGFP vector was a gift from A. Auricchio (Telethon Institute of Genetics and Medicine, Naples). The work was supported by the Deutsche Forschungsgemeinschaft Sonderforschungsbereich 807, Centre of Excellence Frankfurt Macromolecular Complexes, the German Federal Ministry of Education and Research (01GQ0815) and by the EU FP7 OptoNeuro Project (249867) to E.B. and by the Max Planck Society.

AUTHOR CONTRIBUTIONS

E.B., S.K. and P.G.W. conceived the molecular and electrophysiological experiments, and S.K., B.L. and U.T. carried them out. D.G. and C.B. performed the antibody screening. S.K., U.T. and C.B. designed and carried out the data analysis. S.K. and E.B. wrote the paper. E.S.B. supplied the Arch plasmid and contributed to writing.

COMPETING FINANCIAL INTERESTS

The authors declare no competing financial interests.

Published online at http://www.nature.com/naturemethods/.
Reprints and permissions information is available online at http://www.nature.com/reprints/index.html.

1. Nagel, G. *et al.* Light activation of channelrhodopsin-2 in excitable cells of *Caenorhabditis elegans* triggers rapid behavioral responses. *Curr. Biol.* **15**, 2279–2284 (2005).
2. Han, X. & Boyden, E. Multiple-color optical activation, silencing, and desynchronization of neural activity, with single-spike temporal resolution. *PLoS ONE* **2**, e299 (2007).
3. Zhang, F. *et al.* Multimodal fast optical interrogation of neural circuitry. *Nature* **446**, 633–639 (2007).
4. Douin, V. *et al.* Use and comparison of different internal ribosomal entry sites (IRES) in tricistronic retroviral vectors. *BMC Biotechnol.* **4**, 16 (2004).
5. Han, X., Qian, X., Stern, P., Chuong, A. & Boyden, E. Informational lesions: optical perturbation of spike timing and neural synchrony via microbial opsin gene fusions. *Front. Mol. Neurosci.* **2**, 12 (2009).
6. Tang, W. *et al.* Faithful expression of multiple proteins via 2A-peptide self-processing: a versatile and reliable method for manipulating brain circuits. *J. Neurosci.* **29**, 8621–8629 (2009).
7. de Felipe, P. *et al.* E unum pluribus: multiple proteins from a self-processing polyprotein. *Trends Biotechnol.* **24**, 68–75 (2006).
8. Gradinaru, V. *et al.* Molecular and cellular approaches for diversifying and extending optogenetics. *Cell* **141**, 154–165 (2009).
9. Geibel, S. *et al.* The voltage-dependent proton pumping in bacteriorhodopsin is characterized by optoelectic behavior. *Biophys. J.* **81**, 2059–2068 (2001).
10. Seki, A. *et al.* Heterologous expression of *Pharaonis halorhodopsin* in *Xenopus laevis* oocytes and electrophysiological characterization of its light-driven Cl^- pump activity. *Biophys. J.* **92**, 2559–2569 (2007).
11. Nagel, G., Möckel, B., Büldt, G. & Bamberg, E. Functional expression of bacteriorhodopsin in oocytes allows direct measurement of voltage dependence of light induced H^+ pumping. *FEBS Lett.* **377**, 263–266 (1995).
12. Shcherbo, D. *et al.* Bright far-red fluorescent protein for whole-body imaging. *Nat. Methods* **4**, 741–746 (2007).
13. Feldbauer, K. *et al.* Channelrhodopsin-2 is a leaky proton pump. *Proc. Natl. Acad. Sci. USA* **106**, 12317–12322 (2009).
14. Zufferey, R. *et al.* Self-inactivating lentivirus vector for safe and efficient *in vivo* gene delivery. *J. Virol.* **72**, 9873–9880 (1998).
15. Bamann, C., Gueta, R., Kleinlogel, S., Nagel, G. & Bamberg, E. Structural guidance of the photocycle of channelrhodopsin-2 by an interhelical hydrogen bond. *Biochemistry* **49**, 267–278 (2010).
16. Berndt, A., Yizhar, O., Gunaydin, L., Hegemann, P. & Deisseroth, K. Bi-stable neural state switches. *Nat. Neurosci.* **12**, 229–234 (2009).
17. Zhang, F. *et al.* Red-shifted optogenetic excitation: a tool for fast neural control derived from *Volvox carteri*. *Nat. Neurosci.* **11**, 631–633 (2008).
18. Chizhov, I. & Engelhard, M. Temperature and halide dependence of the photocycle of halorhodopsin from *Natronobacterium pharaonis*. *Biophys. J.* **81**, 1600–1612 (2001).
19. Lanyi, J. Halorhodopsin: A light-driven chloride ion pump. *Annu. Rev. Biophys. Biophys. Chem.* **15**, 11–28 (1986).
20. Dencher, N. & Wilms, M. Flash photometric experiments on the photochemical cycle of bacteriorhodopsin. *Biophys. Struct. Mech.* **1**, 259–271 (1975).
21. Chow, B. *et al.* High-performance genetically targetable optical neural silencing by light-driven proton pumps. *Nature* **463**, 98–102 (2010).
22. Kleinlogel, S. *et al.* Ultra light-sensitive and fast neuronal activation with the $Ca2^+$-permeable channelrhodopsin CatCh. *Nat. Neurosci.* **14**, 513–518 (2011).
23. Yang, F., Moss, L. & Phillips, G. The molecular structure of green fluorescent protein. *Nat. Biotechnol.* **14**, 1246–1251 (1996).
24. Patterson, G. & Lippincott-Schwartz, J. A photoactivatable GFP for selective photolabeling of proteins and cells. *Science* **297**, 1873–1877 (2002).
25. Nagel, G. *et al.* Channelrhodopsin-2, a directly light-gated cation-selective membrane channel. *Proc. Natl. Acad. Sci. USA* **100**, 13940–13945 (2003).
26. Hackmann, C. *et al.* Static and time-resolved step-scan Fourier transform infrared investigations of the photoreaction of halorhodopsin from *Natronobacterium pharaonis*: consequences for models of the anion translocation mechanism. *Biophys. J.* **81**, 394–406 (2001).
27. Hegemann, P., Oesterhelt, D. & Bamberg, E. The transport activity of the light-driven chloride pump halorhodopsin is regulated by green and blue light. *Biochim. Biophys. Acta* **819**, 195–205 (1985).

ONLINE METHODS

Animals. All procedures were performed in accordance with the guidelines from the Max Planck Society and approved by local authorities (Regierungspräsidium Darmstadt). All animals were obtained from the Max Planck Institute for Brain Research (Frankfurt).

Design of the tandem cassette. To form the ChR2-βbR tandem protein, a bacteriorhodopsin construct with an additional N-terminal transmembrane helix was used, termed βbR[9]. The additional transmembrane β segment consists of the first 105 N-terminal amino acids of the rat gastric H^+, K^+-ATPase β subunit (**Supplementary Note 4**) and contains two putative glycosylation sites, which may help the insertion of the tandem protein into the membrane and its stabilization. The *βbR* coding sequence was adapted with suitable primers, isolated by PCR and ligated to the sequence encoding the C terminus of the channelrhodopsin (ChR2-309)-EYFP fusion protein (**Fig. 1a**). The coding sequence of *ChR2-EYFP-βbR* was inserted between the BamHI and HindIII restriction sites of the expression vector pcDNA 3.1(−) (Invitrogen). Subsequently, *βNphR* was adapted with selected primers and PCR and cloned between the SbfI and HindIII restriction sites of the cassette to yield *ChR2-EYFP-βNphR*.

To optimize expression in mammalian cells (i) *ChR2* and bacteriorhodopsin were synthesized with codons optimized for human codon usage (Sloning Biotechnology) and (ii) for optimal utilization of the channel and pump under physiological conditions, the far-red fluorescent protein mKate[12,28] (BioCat; excitation, 588 nm; emmission, 635 nm) was inserted between the SacII and SbfI restriction sites to replace EYFP. The basic *hChR2-mKate-hβbR* was formed and cloned into pcDNA 3.1(−) between the BamHI and HindIII restriction sites. Site-directed mutagenesis (QuikChange, Stratagene) was used to form *hChR2(H134R)-mKate-hβbR*, *hChR2(C128A)-mKate-hβbR* and *hChR2(D156A)-mKate-hβbR*.

In a similar manner *hVChR1-mKate-βhChR2* was constructed with humanized versions of *VChR1(1–300)*[17] and *ChR2(1–348)* (Sloning Biotechnology), but in the order hVChR1-mKate-hChR2. Mutations to mKate were introduced to increase fluorescence at physiological pH[28]. The tandem *hVChR1-mKate-βhChR2(L132C)* was constructed by site-directed mutagenesis (QuikChange, Stratagene) of *hVChR1-mKate-βhChR2* and *ChR2-EYFP-βArch* by linearization of *ChR2-EYFP-βNphR* with BspEI and HindIII and subsequent ligation with the PCR-amplified *Arch* gene[21]. All open reading frames are available in the **Supplementary Note 4**.

Recombinant adeno-associated viral vector construction. Owing to the restricted packaging capacity of rAAVs (~4.7 kb except rAAV2/5 ~8.9 kb (ref. 29)), promoter length in combination with tandem plasmids is limited. The presented rhodopsin fusion proteins with maximal lengths of 3 kb (**Fig. 1b**), however, leave enough space in the rAAV cassette to be combined with common neuronal promoters. If promoter length becomes an issue, long cell-specific promoters can be replaced by small (100–500 bp) cell-specific regulatory enhancer regions in combination with minimal core promoter sequences or the use of ligand-associated rAAV capsids that bind to cell surface receptors unique to the target cells[30]. We used a short 454 bp HIV-LTR enhancer-promoter sequence[14] (kind gift from V. Busskamp, sequence given in **Supplementary Note 4**), which mainly labeled neurons in hippocampal cell cultures contrary to the initially used CMV promoter, which chiefly labeled glial cells. The PCR-amplified LTR promoter sequence was cut by NheI and PstI and inserted into *pAAV2-Rho-EGFP*[31] to obtain *pAAV2-LTR-EGFP*. This viral expression plasmid contained additionally a woodchuck post-transcriptional regulatory element (*WPRE*) and a bovine growth hormone (*BGH*) polyadenylation sequence. The coding sequence of *ChR2-EYFP-βbR*, *ChR2-EYFP-βNphR*, *hChR2(H134R)-mKate-hβbR* and *hVChR1-mKate-βhChR2* were PCR-amplified and subcloned into *pAAV2-LTR-EGFP* by replacement of *EGFP*. The cloning was performed with Clontech's In-Fusion kit, since unique restriction sites for conventional cloning strategies are missing. *pAAV2-LTR-EGFP* was linearized by PstI and BamHI and the optimized Kozak sequence was set upstream of the start codon. The viral vectors (pAAV2-LTR-Tx; Tx refers to the above mentioned tandem constructs) were packaged (serotype 7) and affinity purified at the Gene Therapy Program of the University of Pennsylvania with final infectious virus titers of 4×10^{12} to 7×10^{12} genome copies per ml.

HEK293 and neuroblastoma (NG108-15) cell cultures and transfection. HEK293 (ATCC: CRL-1573) and NG108-15 (ATCC: HB-12317) cells were maintained in Dulbecco's Modified Eagle Medium (PAA; high-glucose, with GlutaMax) supplemented with 10% FCS, 10 U ml^{-1} penicillin and 100 µg ml^{-1} streptomycin. To induce differentiation of NG108-15 cells, 100 µl 1 × N2 supplement (Gibco), 2 µM forskolin and 200 µM dibutyryl cAMP (Sigma) were added to the culture medium 5–7 d before the experiment. Twenty-four to forty-eight hours before the electrophysiological recordings, HEK293 and NG108-15 were transiently transfected using Effectene (Qiagen), Lipofectamine 2000 (Invitrogen) or Promofectin-Neuron (PromoKine) and 1 µM of all-*trans* retinal added to the culture medium. In addition a HEK293 FlpIn T-Rex hVChR1-mKate-βhChR2 cell line was generated and kept under hygromycin (100 µg ml^{-1}) and blasticidin (15 µg ml^{-1}) selection. Protein-expression was initiated 24 h before measurements by addition of 1 µg ml^{-1} tetracycline.

Hippocampal neuron cultures and rAAV transduction. Hippocampi were isolated from embryonic E18 Sprague-Dawley rats (Jackson Laboratory) and treated with papain (20 U ml^{-1}) for 20 min at 37 °C. The hippocampi were washed with DMEM (Invitrogen/Gibco, high glucose) and titrated in DMEM supplemented with 10% FBS. Approximately 75,000 cells in 750 µl medium were plated on poly(D-lysine) and laminin coated glass cover slips in 24-well plates. After 3 h DMEM was replaced by culture medium (Neurobasal containing 2% B-27 supplement, 2 mM glutamax-I and 100 U ml^{-1} penicillin and 100 µg ml^{-1} streptomycin). Five days after plating, 5×10^{10} or 1×10^{11} GC ml^{-1} of virus rAAV2/7.Tx.WPRE.bGH was added to each well. Expression became visible 10 d after transduction. No neurotoxicity was observed for the lifetime of the culture (~4 weeks). No all-trans retinal was added to the culture medium or recording medium for any of the experiments described here.

Electrophysiology. Patch pipettes with resistances of 2–4 MΩ for HEK293 cells and 4–10 MΩ for NG108-15 cells and hippocampal

neurons were fabricated from thick-walled borosilicate glass (GB150F-8P, Science Products) on a horizontal DMZ-Universal puller (Zeitz Instruments). The pipette solution for HEK293 cells and undifferentiated NG108-15 cells contained 110 mM NaCl, 2 mM $MgCl_2$, 10 mM EGTA and 10 mM HEPES (pH 7.4). The bath solution was 140 mM NaCl, 2 mM $MgCl_2$, 2 mM $CaCl_2$ and 10 mM HEPES (pH 7.4). For measurements on hVChR1-βhChR2 expressing NG108-15 cells the pipette solution contained 130 mM K-gluconate, 2 mM $MgCl_2$, 1 mM EGTA, and 15 mM HEPES (pH 7.2) and the bath solution 140 mM NaCl, 3.5 mM KCl, 2 mM $MgCl_2$, 2 mM $CaCl_2$, 10 mM glucose and 10 mM HEPES (pH 7.4). For differentiated NG108-15 cells and cultured hippocampal neurons the intracellular solution contained 3 mM NaCl, 10 mM HEPES, 10 mM EGTA, 110 mM D-gluconic acid, 1 mM $CaCl_2$, 1 mM $MgCl_2$, 1 mM ATP_{Na2}, 1 mM ATP_{Mg} and 1mM GTP_{Na} (pH 7.3). Tyrode's solution (125 mM NaCl, 2 mM KCl, 2 mM $CaCl_2$, 1 mM $MgCl_2$, 30 mM glucose and 25 mM HEPES, pH 7.4) complemented by the excitatory synaptic transmission blockers NBQX (1,2,3,4-tetrahydro-6-nitro-2,3-dioxo-benzo[f]quinoxaline-7-sulfonamide, Sigma, 10 μM) and AP-5 (D(−)-2-amino-5-phosphonopentanoic acid, Sigma, 50 μM) was employed as the extracellular solution. Recordings were conducted on an inverted Zeiss Axiovert 25 microscope equipped with a fluorescence lamp and successful protein expression was verified by EYFP- or mKate-mediated fluorescence. Neuronal access resistances were 15–40 MΩ and were monitored for stability throughout the experiments. Electrophysiological signals were amplified using either an Axopatch 200A (Axon Instruments) or a PC 7 (HEKA) patch clamp amplifier, filtered at 2 kHz (HEK293), 5 kHz (HEK293 FlpIn T-Rex hVChR1-mKate-βhChR2) and 10 kHz (NG108-15 cells, neurons), digitized with an Axon Digidata (1200, 1320 or 1400, Molecular Devices) and acquired and analyzed using pClamp9 or pClamp10 software (Molecular Devices).

Light sources. In most experiments light-pulses were produced by diode-pumped solid-state lasers (PuschOpto Tech; λ_1 = 473 nm, λ_2 = 532 nm, λ_3 = 593.5 nm) combined with fast computer-controlled shutters. The Uniblitz LS6 shutter used in combination with the 593 nm laser has a closing time constant of 1.3 ms, which may slightly decelerate the steady-state decay time measurements for the fast ion pumps NphR and Arch. The three lasers were coupled into a single 400 μm diameter quartz optic fiber (STE-F100/400-Y-VIS/NIR; Laser 2000) and intensity outputs were equilibrated to equal, saturating photon densities before each experiment (specific light intensities are indicated in the figure legends and are intensities at the end of the optic fiber at a distance of ~500 μm from the cell). Time-resolved measurements of opening kinetics (single turnover measurements) were performed with 10 ns light-pulses from an excimer-pumped dye laser (λ_1 = 399 nm, 2-(1,1′-biphenyl)-4-yl-6-phenyl-benzoxazole (PBBO); λ_2 = 500 nm, coumarin 307; λ_3 = 580 nm rhodamine 6G; J ~20 μJ). For action spectra a 1000W XBO lamp (Cool 1000; Müller) in combination with a fast shutter (LS2T2-NL, Vincent Associates), narrow band interference filters (bandwidth 10 ± 2 nm; Andover Corporation) and neutral density filters was used to achieve constant photon-density illumination at different wavelengths. For hVChR1-mKate-βhChR2, adjustments for the reduced peak current contribution of hVChR1 compared to hChR2 were required before fitting.

Confocal imaging. Coverslips were fixed at 4 °C for 10 min in 4% paraformaldehyde in PBS buffer containing 2% sucrose. The cells were subsequently incubated for 1.5 h in rabbit antibody to GFP (anti-GFP IgG; Invitrogen, A11122) or rabbit antibody to mKate (anti-mKATE IgG; BioCat, AB231-EV) followed by a 45-min incubation in Alexa Fluor 488–conjugated donkey anti-rabbit (Invitrogen, A21206). Immunofluorescence of mounted coverslips was photographed using a Zeiss AxioExiner ApoTome fluorescence microscope or a Zeiss LSM 510 confocal microscope.

Antibody generation, epitope characterization and western blot analysis. For the antibody production, mice were immunized with purified ChR2(315), sacrificed to isolate the spleen and antibodies collected from hybridoma cell sera (mfd Diagnostics). Antibody performance and epitope characterization were tested with immunocytochemical, immunohistochemical and western blot analyses. The results are summarized in the **Supplementary Figure 2** and **Supplementary Note 1**.

Immunocytochemistry. Stably ChR2(1–309)-EYFP–expressing HEK293 cells were fixed with 100% methanol (−20 °C, 10 min) and subsequently permeabilized with acetone (−20 °C, 10 min). Nonspecific binding surface was blocked using 2.5% normal goat serum in PBS. The cells were immunostained with an antibody to ChR2 (anti-ChR2; 1:100 in blocking solution) and an Alexa Fluor 546–conjugated goat-anti-mouse secondary antibody (1:5,000, Invitrogen). The pictures were taken with an Axio Imager fluorescence microscope (Zeiss) by using a 64× oil-immersion objective.

Immunohistochemistry. For immunohistochemical analysis, paraformaldehyde-fixed 14 μm-thick transverse retinal cryosections were obtained either from a transgenic mouse expressing *ChR2-EYFP* under the *Thy1* promoter (+)[32,33] or from a non-ChR2-expressing mouse. For immunohistochemical labeling, the αChR2 antibody and an Alexa Fluor 546–conjugated goat-anti-mouse secondary antibody were used. The fluorescence signal of the ChR2-EYFP fusion protein was amplified using a rabbit anti-GFP (1:200, ABfinity, Invitrogen) and an Alexa Fluro 488–conjugated goat anti-rabbit secondary (1:5,000, Invitrogen). The pictures were taken using an Axio Imager fluorescence microscope with a 10× air and a 64× oil-immersion objective.

Epitope mapping. The epitope between amino acids 290 and 309 was located by western blot analyses from Triton X-100 lysates of oocytes expressing different constructs. Chimeras between ChR1 and ChR2 were constructed, either linking the transmembrane helices 1–3 (residues 1–180) from ChR1 with the helices 4–7 (residues 142–315) from ChR2 (construct C1), or linking transmembrane helices 1–2 (residues 1–148) from ChR1 with the helices 3–7 (residues 112–315) from ChR2 (construct C2). Additional fusion proteins between the C terminus of ChR2 and EYFP were constructed (ChR2(270–309)-EYFP; ChR2(285–309)-EYFP). Functional expression was tested 3 d after mRNA injection by two-electrode voltage clamp or detection of yellow fluorescence.

Protein extraction and western blot analysis. Eighteen hours after transient transfection HEK293 cells were collected with lysis buffer, containing 0.5% Nonidet P40 in 1× PBS (with protease

doi:10.1038/nmeth.1766

inhibitors, Roche Complete). Total cell lysate (30–110 µg per lane) was separated by SDS-PAGE (10%, NuPAGE^R, Invitrogen), transferred to nitrocellulose membranes electrophoretically overnight at 4 °C (x-cell, Invitrogen). Western blots were probed with an anti-GFP (1:100; rabbit IgG fraction, Clontech) and a monoclonal anti-ChR2 (1:500). The secondary immunoreactions were performed using a horseradish-peroxidase–conjugated goat anti-rabbit (1:3,000; Biotechnology) or anti-mouse (1:3,000; BioRad), respectively. The blots were incubated in 4-chloro-1-naphthol and 3,3′-diaminobenzidine tetrahydrochloride (CN and DAB) Substrate (Thermo Fisher Scientific) for 5 min until specific bands became visible. Scanned images were enhanced in contrast and brightness (Adobe Photoshop 7).

Calculation of copy number and pump ion-turnover rate. We compared calculated pump turnovers for different rhodopsins (**Table 1**) by taking the correction factor f_D for the ChR2 desensitization into account (**Supplementary Note 5**). The copy number density (N) is defined as:

$$N_{\mathrm{ChR2\_pump}} = \frac{f_D \times I(\mathrm{ChR2})_{\mathrm{stat}}}{i_{\mathrm{ChR2}} \times P_{\mathrm{oRT,140\,mM}}} \times C_m,$$

where $I(\mathrm{ChR2})_{\mathrm{stat}}$ denotes the ChR2 steady-state current densities in pA per pF from **Table 1**, i_{ChR2} the ChR2 single channel current at −60 mV and room temperature (RT; 22 °C; $i = -2.385 \pm 0.8$ fA, mean ± s.d.) calculated from the single channel conductance extrapolated to 140 mM sodium concentration ($\gamma(\mathrm{ChR2})_{\mathrm{RT,\,140\,mM}} = \gamma(\mathrm{ChR2(H134R)})_{\mathrm{RT,\ 140\ mM}} = 39.7 \pm 13.7$ fS, mean ± s.d.)[13]. In addition, $P_{\mathrm{oRT,140\,mM}}$ denotes the open probability extrapolated for 140 mM sodium and room temperature ($P_o(\mathrm{ChR2}_{\mathrm{RT,\,140\,mM}}) = 0.58 \pm 0.23$, mean ± s.d.; $P_o(\mathrm{ChR2(H134R)}_{\mathrm{RT,\ 140\ mM}}) = 0.66 \pm 0.14$, mean ± s.d.)[13], while C_m corresponds to the specific membrane capacitance of HEK293 cells (1.15 µF cm^{-2})[34]. The correction factors (f_D) are 2.7 for ChR2 and 1.9 for hChR2(H134R) (**Supplementary Note 5**).

The pump ion-turnover rate (x) is defined as:

$$x = \frac{I(\mathrm{pump})_{\mathrm{stat}} \times C_m}{N_{\mathrm{ChR2\_pump}} \times e_0}$$

with $I(\mathrm{pump})_{\mathrm{stat}}$ representing the current densities from **Table 1** and e_0 the elementary charge.

28. Pletnev, S. *et al.* A crystallographic study of bright far-red fluorescent protein mKate reveals pH-induced cis-trans isomerization of the chromophore. *J. Biol. Chem.* **283**, 28980–28987 (2008).
29. Allocca, M. *et al.* Serotype-dependent packaging of large genes in adeno-associated viral vectors results in effecive gene delivery in mice. *J. Clin. Invest.* **118**, 1955–1964 (2008).
30. Büning, H. *et al.* Receptor targeting of adeno-associated virus vectors. *Gene Ther.* **10**, 1142–1151 (2003).
31. Allocca, M. *et al.* Novel adeno-associated virus serotypes efficiently transduce murine photoreceptors. *J. Virol.* **81**, 11372–11380 (2007).
32. Arenkiel, B. *et al. In vivo* light-induced activation of neural circuitry in transgenic mice expressing channelrhodopsin-2. *Neuron* **54**, 205 (2007).
33. Thyagarajan, S. *et al.* Visual function in mice with photoreceptor degeneration and transgenic expression of channelrhodopsin 2 in ganglion cells. *J. Neurosci.* **30**, 8745 (2010).
34. Zimmermann, D. *et al.* Effects on capacitance by overexpression of membrane proteins. *Biochem. Biophys. Res. Commun.* **369**, 1022–1026 (2008).

Nature Methods

A gene-fusion strategy for stoichiometric and co-localized expression of light-gated membrane proteins

Sonja Kleinlogel[1], Ulrich Terpitz, Barbara Legrum[1], Deniz Gökbuget[1,4], Edward S Boyden[2], Christian Bamann[1], Phillip G Wood[1] & Ernst Bamberg

Supplementary Figure 1	Absorption cross-section of ChR2 and pumps.
Supplementary Figure 2	Immunohistochemical characterization and epitope mapping of the monoclonal ChR2 antibody (αChR2).
Supplementary Figure 3	Light-intensity tuning of ChR2-βbR in neuroblastoma cells.
Supplementary Figure 4	Kinetic tuning of slow-mutant tandems expressed in HEK293 cells.
Supplementary Figure 5	Pump current-to-voltage relationships.
Supplementary Figure 6	Single turnover measurements on HEK293 FlpIn T-Rex hVChR1-βhChR2 cells.
Supplementary Note 1	Antibody generation, antibody performance and epitope mapping.
Supplementary Note 2	Kinetic properties of the ion-pumps bR, NphR and Arch expressed in HEK293 cells.
Supplementary Note 3	Current levels and kinetics of hVChR1-βhChR2 *vs.* hChR2 and hVChR1 transiently expressed in cultured neuroblastoma cells.
Supplementary Note 4	Sequence information.
Supplementary Note 5	Consideration of the ChR2 desensitization for ion-turnover calculations

Supplementary Figure 1

Absorption cross-section of ChR2 and pumps.

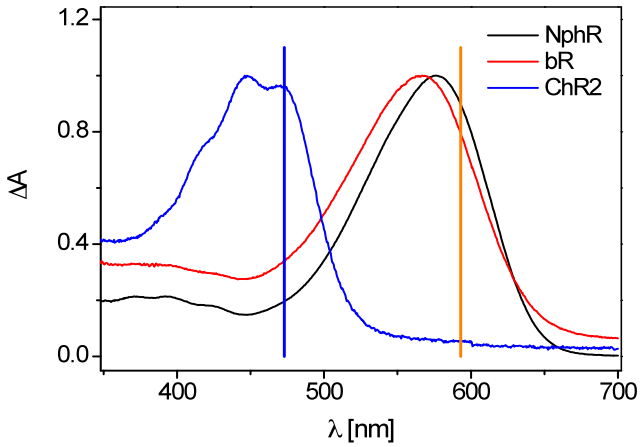

The absorption cross-section of the ion pumps NphR and bR amount to 20-30% compared to that of ChR2 at 473-nm illumination. Each channelrhodopsin-pump tandem construct has to be calibrated in terms of potential spectral overlap at the activation wavelengths chosen, which can potentially shift the reversal potential of the single proteins and modify the excitation-to-inhibition current ratios important for controlled, calibrated membrane potential tuning. Under the illumination conditions of **Fig. 1d**, both rhodopsins are in saturation and we can simply apply an apparent tandem reversal potential, where $I_{pump} = I_{ChR2}$. For ChR2-EYFP-βNphR it is shifted to more negative values than for ChR2-EYFP-βbR. Similarly, in hVChR1-mKate-βhChR2 and hVChR1-mKate-βhChR2(L132C), hVChR1 is co-activated with hChR2 (**Fig. 3b**) and CatCh, respectively, under 473-nm illumination, thus increasing the measured hChR2 and CatCh currents and leading to an underestimation of CatCh's single channel conductance.

Supplementary Figure 2

Immunohistochemical characterization and epitope mapping of the monoclonal mouse anti-ChR2 antibody (αChR2). For additional discussion see Supplementary Note 1.

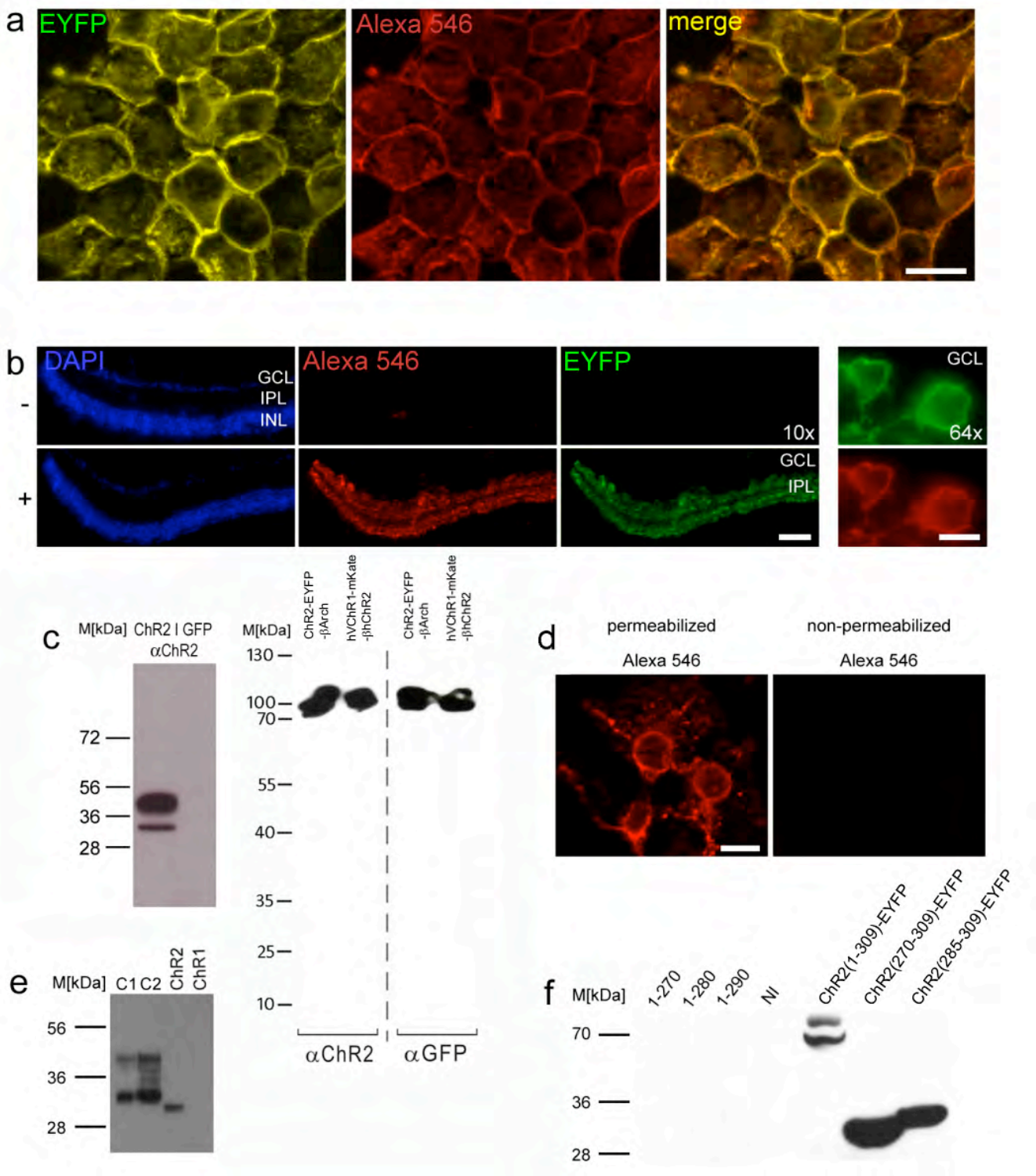

(**a**) Immunostaining of cultured ChR2(1-309)-EYFP expressing HEK293 cells with anti-ChR2 mouse antibody (αChR2; 1:100 in blocking solution) and an Alexa-546 conjugated goat anti-mouse secondary antibody (1:5000, Invitrogen). Scale bar 10 μm. (**b**) Immunohistochemical labeling with αChR2 and an Alexa-546 conjugated goat anti-mouse secondary antibody of retinal cryosections from a transgenic mouse expressing ChR2-EYFP (+) and a non-ChR2-expressing mouse (-). The ganglion cell layer (GCL) and inner nuclear layer (INL), in-between which lies the inner plexiform layer (IPL) containing the ganglion cell axons, are visualized with 4',6-diamidino-2-phenylindole (DAPI). The signal for EYFP was enhanced by labeling with an anti-GFP antibody and an Alexa-488 conjugated secondary antibody. Scale bars are 50 μm at 10x magnification and 10 μm at 64x magnification. (**c**) Left, Western blot data on cell lysates form HEK293 cells transiently expressing ChR2(1-309) or GFP to exclude αChR2 immunoreactivity toward EYFP. αChR2 detected the ~34 kDa ChR2 protein only in the cell lysate from ChR2-expressing HEK cells (the larger band belongs to the glycosylated ChR2 protein) but not in the lysate from GFP-expressing HEK cells. Right, Western blots of cell lysates of HEK293 cells transfected with the tandems *ChR2-EYFP-βArch* and *hvChR1-mKate-βhChR2*. αChR2 and αGFP detected the ~100 kDa bands of the intact fusion proteins. (**d**) Immunocytochemical staining of permeabilized and non-permeabilized HEK293 cells stably expressing ChR2(1-309)-EYFP. Only permeabilized cells show αChR2 labeling, indicating that the epitope is located intracellularly (scale bar 5 μm). (**e**) First step of epitope mapping. Western Blot with αChR2 on lysates from oocytes expressing channelrhodopsin chimeras C1 (ChR1(1-180)-ChR2(142-315)) and C2 (ChR1(1-148)-ChR2(112-315)). ChR2 and ChR1-injected oocytes were used as controls. (**f**) Second step of epitope mapping using oocyte injections with C-terminally truncated ChR2 constructs (1-270, 1-280, 1-290) and C-terminal peptide fragments of ChR2 fused to EYFP (ChR2(270-309)-EYFP and ChR2(285-309)-EYFP). Epitope recognition was tested in a Western blot with αChR2 showing no recognition of the truncated constructs but bands for constructs ChR2(270-309)-EYFP and ChR2(285-309)-EYFP, indicating that the αChR2 epitope is located between amino acids 290 and 309 of ChR2. Non-injected oocytes (NI) and the full-length ChR2(1-309)-EYFP fusion protein were used as controls.

Supplementary Figure 3

Light-intensity tuning of ChR2-EYFP-βbR in neuroblastoma cells.

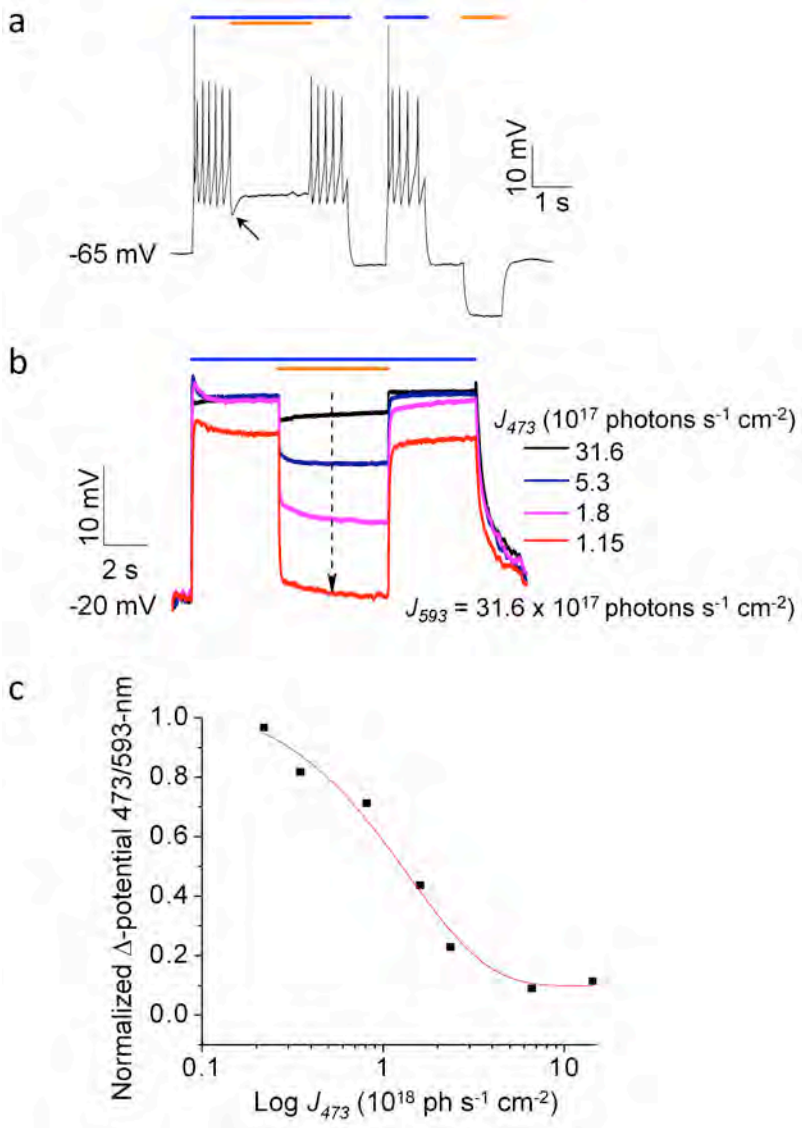

(**a**) Representative current clamp recording from a differentiated neuroblastoma NG108-15 cell transiently transfected with ChR2-EYFP-βbR. 473-nm light (3.5×10^{19} photons s^{-1} cm^{-2}) induced spiking and concomitant illumination with 593-nm light (2.6×10^{20} photons s^{-1} cm^{-2}) temporally suppressed firing. The arrow indicates a membrane potential trough at orange light onset, indicative of initial strong hyperpolarization induced by the bR peak current. Bars indicate photostimulation. (**b**) Light intensity tuning under blue (473 nm) and orange (593 nm) double illumination condition: The blue-light intensity was tuned (arrow) for optimal cancellation of the blue-light induced depolarization by additional orange-light in a non-differentiated NG108-15 cell. The illumination protocol is indicated by the colored bars. (**c**) 473-nm light-intensity-tuning curve for optimal 593-nm

depolarization cancellation during 473/593-nm double illumination of another non-differentiated NG108-15 cell. The 593-nm intensity was set to 6.6×10^{18} photons s^{-1} cm^{-2} and the 473-nm intensity was stepwise increased from $1/30^{th}$ of the 593-nm intensity (2.2×10^{17} photons s^{-1} cm^{-2}, leading to optimal depolarization cancellation) to over 6.6×10^{18} photons s^{-1} cm^{-2} (leading to minimal depolarization cancellation). The fractional depolarization ($\Delta = \left| \frac{V_{473nm}(ph) - V_{593nm}}{V_{473nm}(ph) - V_{dark}} \right|$) measured under double illumination conditions (V_{593nm}) is plotted in dependence of the 473-nm induced depolarization at different light intensities ($V_{473nm}(ph)$) normalized to the resting potential in the dark (V_{dark}).

Supplementary Figure 4

Kinetic tuning of slow-mutant tandems expressed in HEK293 cells.

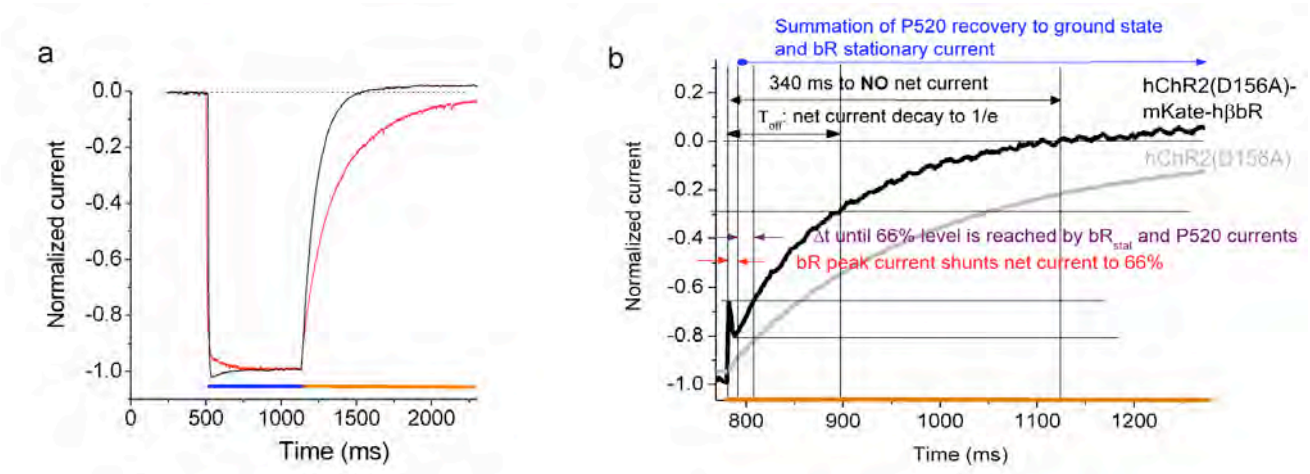

(**a**) By combination of hChR2(C128A) with hβbR (black trace) the apparent orange light OFF-switching is twofold accelerated compared to hChR2(C128A) alone (red trace; measurements at -60 mV) due to simultaneous activation of the ChR2(C128A)-P520 photointermediate and hβbR; the current decay to a specific level is reached faster through the additional hβbR-stationary-current offset. (**b**) Summation of currents in tandem hChR2(D156A)-mKate-hβbR (see **Fig. 3a**) The summation of the hβbR and ChR2-P520 currents reduces the time until no net current is measured by approximately twofold, due to the added outward current offset by hβbR. Additionally, the fast hβbR peak current (τ_{on} ~70 μs, **Supplementary Note 2**) shunts the net current immediately after orange-light onset to about 66% which may suffice (depending on the construct copy number and the excitability of the cell) to hyperpolarize neurons to a subthreshold depolarization level on a submillisecond regime (a 10 ns laser pulse suffices to induce the hβbR peak current) and inhibit

action potential firing immediately, so that ON- and OFF-switching of neuronal firing in hChR2(D156A)-mKate-hβbR may be achieved by brief pulses of blue and orange light.

Supplementary Figure 5

Single turnover measurements on HEK293 FlpIn T-Rex hVChR1-mKate-βhChR2 cells.

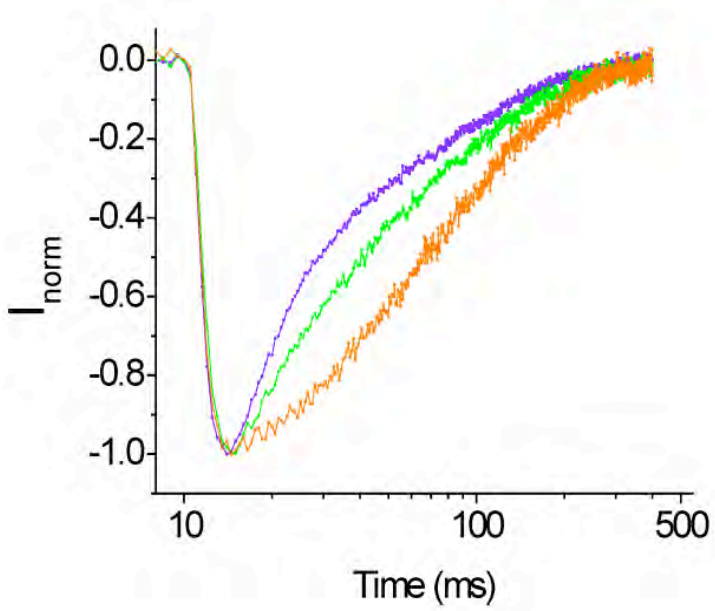

Normalized mean (n=10) photocurrents to 400 nm (violet), 500 nm (green) and 580 nm (orange) 10-ns pulses. With increasing wavelength the relative current contribution of VChR1 increases and slows the closing kinetics.

Supplementary Figure 6

Pump current-to-voltage relationships.

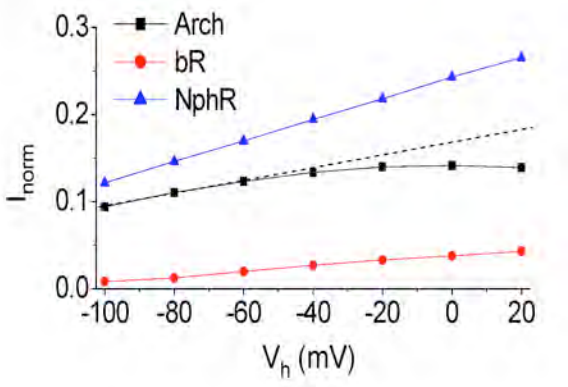

Typical current/voltage relationship of Arch (ChR2-EYFP-βArch) in comparison to bR (ChR2-EYFP-βbR) and NphR (ChR2-EYFP-βNphR). Currents were normalized to the ChR2-currents at -100 mV. Arch currents saturate at positive membrane potentials as opposed to bR and NphR currents.

Supplementary Note 1

Antibody generation, antibody performance and epitope mapping.

Hybridoma cell sera were obtained from mfd Diagnostics (Wendelsheim, Germany) and further tested for identification of hybridoma cell lines showing specific and high cross-reactivity towards ChR2. Cell serum from clone #7 was further used in the characterization as demonstrated in Supplementary Fig. 2. ChR2(1-309)-EYFP expressing HEK293 cells immunostained with the isolated monoclonal mouse anti-ChR2 antibody (αChR2) showed distinct co-localization of the ChR2(1-309)-EYFP fusion protein and αChR2 in the plasma membrane (Supplementary Fig. 2a). Specific co-localization was also observed in retina cryosections from ChR2(1-309)-EYFP expressing mice (Supplementary Fig. 2b). Alexa-546 (corresponding to ChR2) and Alexa-488 (corresponding to EYFP) fluorescence is only seen in the ganglion cell layer (GCL) and the inner plexiform layer (IPL) of the (+)-mouse retina (Supplementary Fig. 2b, lower panels), which expresses ChR2 predominantly in retinal ganglion cells[1]. No fluorescence is observed in mice that do not express ChR2(1-309)-EYFP demonstrating the high specificity of the immunohistochemical staining. To exclude cross-reactivity of αChR2 with the EYFP protein, we transiently transfected HEK293 cells either with *ChR2(1-309)* or with *gfp* alone. Functional expression of the later one was followed by fluorescence. Western Blot analysis ruled out cross-reactivity of the αChR2 with EYFP (Supplementary Fig. 2c, left panel) and corroborates specific detection of ChR2 in the immuno-labelings described above.

For the epitope mapping, we assumed that αChR2 detects a non-membraneous part of the ChR2(1-309). Therefore, we first identified the topology of the epitope by immunostaining of permeabilized and non-permeabilized cells. Only permeabilized cells show αChR2 labeling, indicating that the epitope is located intracellularly (Supplementary Fig. 2d). Next, Western blot analysis with αChR2 showed labeling for ChR2 and C1 and C2 channelrhodopsin chimeras but not for ChR1, revealing that the epitope of αChR2 is located between transmembrane helix 4 and the C-terminus (Supplementary Fig. 2e). Finally, fusion proteins of the C-terminus of ChR2 (residues 285 to 309) and EYFP are detected by αChR2 but not from oocytes injected with mRNA coding for ChR2(1-290) (Supplementary Fig. 2f). Therefore, the location of the epitope resides between amino acids 290 and 309 of ChR2.

Supplementary Note 2

Kinetic properties of the ion-pumps bR, NphR and Arch expressed in HEK293 cells

The additional fast transient outward bR-current upon the onset of orange illumination (**Fig. 1c top**) is indicative of the deprotonation of the Schiff base during the bR proton pump cycle, which does not occur in the NphR chloride pump cycle[2,3]. Activation with 10-ns saturating 580-nm laser pulses (J_{580} ~ 20 μJ) revealed a faster current onset for bR (τ_{on} ~ 70 μs) than for NphR (τ_{on} ~ 300 μs), which is in agreement with spectroscopic photocycle data[3-5] and guarantees a potent onset of bR-mediated light-induced membrane hyperpolarization (**Supplementary Fig. 3a**). After stationary light conditions, the NphR current decays in a mono-exponential process with a time constant (τ_{off}) of 1.8 ± 0.1 ms (mean ± s.e.m., n=4), whereas bR decays in a bi-exponential process with a $\tau_{off}(1)$ of 5.9 ± 0.5 ms (82%) and a $\tau_{off}(2)$ of 123 ± 11 ms (8%, mean ± s.e.m., n=4). The latter, slower relaxation process is indicative of the decay of the M^*-intermediate in a non-transporting photocycle[6].

Single turnover measurements (10-ns pulses, J_{580} ~ 20μJ) on Arch-expressing HEK293 cells revealed fast Arch activation (τ_{on} ~ 50 μs, n=4) similar to that of bR. After stationary light conditions, the Arch current decays in a bi-exponential process with a $\tau_{off}(1)$ of 1.8 ± 0.4 ms (81%) and a $\tau_{off}(2)$ of 20 ± 6 ms (19%, mean ± s.e.m., n=4, table 1), providing further evidence for an accelerated Arch turnover similar to that of NphR. This is valid under the assumption that $\tau_{off}(2)$ represents the slow decay of an M^*–like intermediate in an inactive cycle parallel to the fast active proton pumping cycle, similarly as it occurs in bR[6]. Arch's current-voltage relationship saturates towards positive potentials (**Supplementary Fig. 6**), a behavior never observed in bR[6] or NphR[7,8], suggesting an altered Arch voltage-dependence at high depolarizing potentials.

Supplementary Note 3

Current levels and kinetics of hvChR1-mKate-βhChR2 *vs.* hChR2 and hvChR1 transiently expressed in cultured neuroblastoma cells

At -60 mV, 1-s blue light activation (481 nm, 7.5×10^{16} photons s^{-1} cm^{-2}) led to hVChR1 stationary currents of 10.6 ± 3.0 pA/pF (n=5, mean ± s.e.m.) with a channel closing time constant (τ_{off}) of 95 ± 8 ms (n=4, mean ± s.e.m.) and hChR2 stationary currents of 16 ± 1.5 pA/pF (n=5, mean ± s.e.m.) with a τ_{off} of 10 ± 0.3 ms (n=9, mean ± s.e.m.). In hVChR1-mKate-βhChR2 the simultaneous current contributions of hChR2 and hVChR1 led to current amplitudes between the above values of 12.16 ± 2.5 pA/pF (n=5, mean ± s.e.m.) and a wavelength-dependent apparent τ_{off} being accelerated at short wavelengths (main current contribution from hChR2) and decelerated at long wavelengths (main current contribution from hVChR1). The latter was confirmed by single

turnover measurements on hVChR1-mKate-βhChR2-expressing HEK293 FlpIn T-Rex cells (**Supplementary Fig. 5**; 400 nm, τ_{off} (1) = 10.4 ± 1.0 ms, τ_{off} (2) = 56.3 ± 3.8 ms; 500 nm, τ_{off} (1) = 16.6.± 1.1 ms, τ_{off} (2) = 106.8 ± 5.2 ms; 580 nm τ_{off} (1) 71.1.± 3.5 ms, n=8, mean ± s.e.m.).

Supplementary Note 4

Sequence information

Amino acid sequence (1-105) of the rat gastric H^+,K^+-ATPase β-subunit

MAALQEKKSCSQRMAEFRQYCWNPDTGQMLGRTPARWVWISLYYAAFYVVMTG
LFALCIYVLMQTIDPYTPDYQDQLKSPGVTLRPDVYGERGLQISYNISENSS

HIV-LTR promoter DNA sequence

5'-TTAATGTAGTCTTATGCAATACTCTTGTAGTCTTGCAACATGGTAACGATG
AGTTAGCAACATGCCTTACAAGGAGAGAAAAAGCACCGTGCATGCCGATTGGTG
GAAGTAAGGTGGTACGATCGTGCCTTATTAGGAAGGCAACAGACGGGTCTGACA
TGGATTGGACGAACCACTGAATTGCCGCATTGCAGAGATATTGTATTTAAGTGC
CTAGCTCGATACAATAAACGGGTCTCTCTGGTTAGACCAGATCTGAGCCTGGGA
GCTCTCTGGCTAACTAGGGAACCCACTGCTTAAGCCTCAATAAAGCTTGCCTTG
AGTGCTTCAAGTAGTGTGTGCCCGTCTGTTGTGTGACTCTGGTAACTAGAGATC
CCTCAGACCCTTTTAGTCAGTGTGGAAAATCTCTAGCA-3'

DNA sequence information of reported tandem constructs

CONSTRUCT: *ChR2-EYFP-βbR* (ACCESSION JN836740*)*
CDS *ChR2-EYFP-(HK-β)-bR*/ 1..2721 bp
ChR2 bases 1..927/ amino acids M1--V309 from ACCESSION AF461397
EYFP bases 946..1656/ amino acids V2--Y238 from Clontech Data Sheet
rat *HK-β* bases 1657..1968/ amino acids A2--S105 from ACCESSION M55655
mature-*bR* bases 1972..2718/ amino acids Q1--D249 from ACCESSION V00474

```
  1 ATGGATTATG GAGGCGCCCT GAGTGCCGTT GGGCGCGAGC TGCTATTTGT AACGAACCCA
 61 GTAGTCGTCA ATGGCTCTGT ACTTGTGCCT GAGGACCAGT GTTACTGCGC GGGCTGGATT
121 GAGTCGCGTG GCACAAACGG TGCCCAAACG GCGTCGAACG TGCTGCAATG GCTTGCTGCT
181 GGCTTCTCCA TCCTACTGCT TATGTTTTAC GCCTACCAAA CATGGAAGTC AACCTGCGGC
241 TGGGAGGAGA TCTATGTGTG CGCTATCGAG ATGGTCAAGG TGATTCTCGA GTTCTTCTTC
301 GAGTTTAAGA ACCCGTCCAT GCTGTATCTA GCCACAGGCC ACCGCGTCCA GTGGTTGCGT
361 TACGCCGAGT GGCTTCTCAC CTGCCCGGTC ATTCTCATTC ACCTGTCAAA CCTGACGGGC
421 TTGTCCAACG ACTACAGCAG GCGCACCATG GGTCTGCTTG TGTCTGATAT TGGCACAATT
481 GTGTGGGGCG CCACTTCCGC CATGGCCACC GGATACGTCA AGGTCATCTT CTTCTGCCTG
541 GGTCTGTGTT ATGGTGCTAA CACGTTCTTT CACGCTGCCA AGGCCTACAT CGAGGGTTAC
601 CACACCGTGC CGAAGGGCCG GTGTCGCCAG GTGGTGACTG GCATGGCTTG GCTCTTCTTC
661 GTATCATGGG GTATGTTCCC CATCCTGTTC ATCCTCGGCC CCGAGGGCTT CGGCGTCCTG
```

```
 721 AGCGTGTACG GCTCCACCGT CGGCCACACC ATCATTGACC TGATGTCGAA GAACTGCTGG
 781 GGTCTGCTCG GCCACTACCT GCGCGTGCTG ATCCACGAGC ATATCCTCAT CCACGGCGAC
 841 ATTCGCAAGA CCACCAAATT GAACATTGGT GGCACTGAGA TTGAGGTCGA GACGCTGGTG
 901 GAGGACGAGG CCGAGGCTGG CGCGGTACCC GCGGCCGCCA CCATTGTGAG CAAGGGCGAG
 961 GAGCTGTTCA CCGGGGTGGT GCCCATCCTG GTCGAGCTGG ACGGCGACGT AAACGGCCAC
1021 AAGTTCAGCG TGTCCGGCGA GGGCGAGGGC GATGCCACCT ACGGCAAGCT GACCCTGAAG
1081 TTCATCTGCA CCACCGGCAA GCTGCCCGTG CCCTGGCCCA CCCTCGTGAC CACCTTCGGC
1141 TACGGCCTGC AGTGCTTCGC CCGCTACCCC GACCACATGA AGCAGCACGA CTTCTTCAAG
1201 TCCGCCATGC CCGAAGGCTA CGTCCAGGAG CGCACCATCT TCTTCAAGGA CGACGGCAAC
1261 TACAAGACCC GCGCCGAGGT GAAGTTCGAG GGCGACACCC TGGTGAACCG CATCGAGCTG
1321 AAGGGCATCG ACTTCAAGGA GGACGGCAAC ATCCTGGGGC ACAAGCTGGA GTACAACTAC
1381 AACAGCCACA ACGTCTATAT CATGGCCGAC AAGCAGAAGA ACGGCATCAA GGTGAACTTC
1441 AAGATCCGCC ACAACATCGA GGACGGCAGC GTGCAGCTCG CCGACCACTA CCAGCAGAAC
1501 ACCCCCATCG GCGACGGCCC CGTGCTGCTG CCCGACAACC ACTACCTGAG CTACCAGTCC
1561 GCCCTGAGCA AAGACCCCAA CGAGAAGCGC GATCACATGG TCCTGCTGGA GTTCGTGACC
1621 GCCGCCGGGA TCACTCTCGG CATGGACGAG CTGTACGCAG CCCTGCAGGA GAAGAAGTCA
1681 TGCAGCCAGC GCATGGCCGA ATTCCGGCAA TACTGTTGGA ACCCGGACAC TGGGCAGATG
1741 CTGGGCCGCA CCCCAGCCCG GTGGGTGTGG ATCAGCCTGT ACTATGCAGC TTTCTACGTG
1801 GTCATGACTG GGCTCTTTGC CTTGTGCATC TATGTGCTGA TGCAGACCAT TGATCCCTAC
1861 ACCCCCGACT ACCAGGACCA GTTAAAGTCA CCGGGGGTAA CCTTGAGACC GGATGTGTAT
1921 GGGGAAAGAG GGCTGCAGAT TTCCTACAAC ATCTCTGAAA ACAGCTCTAG ACAGGCCCAG
1981 ATCACCGGAC GTCCGGAGTG GATCTGGCTA GCGCTCGGTA CGGCGCTAAT GGGACTCGGG
2041 ACGCTCTATT TCCTCGTGAA AGGGATGGGC GTCTCGGACC CAGATGCAAA GAAATTCTAC
2101 GCCATCACGA CGCTCGTCCC AGCCATCGCG TTCACGATGT ACCTCTCGAT GCTGCTGGGG
2161 TATGGCCTCA CAATGGTACC GTTCGGTGGG GAGCAGAACC CCATCTACTG GGCGCGGTAC
2221 GCTGACTGGC TGTTCACCAC GCCGCTGTTG TTGTTAGACC TCGCGTTGCT CGTTGACGCG
2281 GATCAGGGAA CGATCCTTGC GCTCGTCGGT GCCGACGGCA TCATGATCGG GACCGGCCTG
2341 GTCGGCGCAC TGACGAAGGT CTACTCGTAC CGCTTCGTGT GGTGGGCGAT CAGCACCGCA
2401 GCGATGCTGT ACATCCTGTA CGTGCTGTTC TTCGGGTTCA CCTCGAAGGC CGAAAGCATG
2461 CGCCCCGAGG TCGCATCCAC GTTCAAAGTA CTGCGTAACG TTACCGTTGT GTTGTGGTCC
2521 GCGTATCCCG TCGTGTGGCT GATCGGCAGC GAAGGTGCGG GAATCGTGCC GCTGAACATC
2581 GAGACGCTGC TGTTCATGGT GCTTGACGTG AGCGCGAAGG TCGGCTTCGG GCTCATCCTC
2641 CTGCGCAGTC GTGCGATCTT CGGCGAAGCC GAAGCGCCGG AGCCGTCCGC CGGCGACGGC
2701 GCGGCCGCGA CCAGCGACTG A
//
```

CONSTRUCT:	*ChR2-EYFP-βNphR* (ACCESSION JN836741)
CDS	*ChR2-EYFP-(HK-β)-NphR*/ 1..2871 bp
ChR2	bases 1..927/ amino acids M1--V309 from ACCESSION AF461397
EYFP	bases 946..1656/ amino acids V2--Y238 from Clontech Data Sheet
rat *HK-β*	bases 1657..1968/ amino acids A2--S105 from ACCESSION M55655
NphR	bases 1999..2868/ amino acids T2--D291 from ACCESSION J05199

```
   1 ATGGATTATG GAGGCGCCCT GAGTGCCGTT GGGCGCGAGC TGCTATTTGT AACGAACCCA
  61 GTAGTCGTCA ATGGCTCTGT ACTTGTGCCT GAGGACCAGT GTTACTGCGC GGGCTGGATT
 121 GAGTCGCGTG GCACAAACGG TGCCCAAACG GCGTCGAACG TGCTGCAATG GCTTGCTGCT
 181 GGCTTCTCCA TCCTACTGCT TATGTTTTAC GCCTACCAAA CATGGAAGTC AACCTGCGGC
 241 TGGGAGGAGA TCTATGTGTG CGCTATCGAG ATGGTCAAGG TGATTCTCGA GTTCTTCTTC
 301 GAGTTTAAGA ACCCGTCCAT GCTGTATCTA GCCACAGGCC ACCGCGTCCA GTGGTTGCGT
 361 TACGCCGAGT GGCTTCTCAC CTGCCCGGTC ATTCTCATTC ACCTGTCAAA CCTGACGGGC
 421 TTGTCCAACG ACTACAGCAG GCGCACCATG GGTCTGCTTG TGTCTGATAT TGGCACAATT
 481 GTGTGGGGCG CCACTTCCGC CATGGCCACC GGATACGTCA AGGTCATCTT CTTCTGCCTG
 541 GGTCTGTGTT ATGGTGCTAA CACGTTCTTT CACGCTGCCA AGGCCTACAT CGAGGGTTAC
 601 CACACCGTGC CGAAGGGCCG GTGTCGCCAG GTGGTGACTG GCATGGCTTG GCTCTTCTTC
 661 GTATCATGGG GTATGTTCCC CATCCTGTTC ATCCTCGGCC CCGAGGGCTT CGGCGTCCTG
 721 AGCGTGTACG GCTCCACCGT CGGCCACACC ATCATTGACC TGATGTCGAA GAACTGCTGG
 781 GGTCTGCTCG GCCACTACCT GCGCGTGCTG ATCCACGAGC ATATCCTCAT CCACGGCGAC
 841 ATTCGCAAGA CCACCAAATT GAACATTGGT GGCACTGAGA TTGAGGTCGA GACGCTGGTG
```

```
 901 GAGGACGAGG CCGAGGCTGG CGCGGTACCC GCGGCCGCCA CCATTGTGAG CAAGGGCGAG
 961 GAGCTGTTCA CCGGGGTGGT GCCCATCCTG GTCGAGCTGG ACGGCGACGT AAACGGCCAC
1021 AAGTTCAGCG TGTCCGGCGA GGGCGAGGGC GATGCCACCT ACGGCAAGCT GACCCTGAAG
1081 TTCATCTGCA CCACCGGCAA GCTGCCCGTG CCCTGGCCCA CCCTCGTGAC CACCTTCGGC
1141 TACGGCCTGC AGTGCTTCGC CCGCTACCCC GACCACATGA AGCAGCACGA CTTCTTCAAG
1201 TCCGCCATGC CCGAAGGCTA CGTCCAGGAG CGCACCATCT TCTTCAAGGA CGACGGCAAC
1261 TACAAGACCC GCGCCGAGGT GAAGTTCGAG GGCGACACCC TGGTGAACCG CATCGAGCTG
1321 AAGGGCATCG ACTTCAAGGA GGACGGCAAC ATCCTGGGGC ACAAGCTGGA GTACAACTAC
1381 AACAGCCACA ACGTCTATAT CATGGCCGAC AAGCAGAAGA ACGGCATCAA GGTGAACTTC
1441 AAGATCCGCC ACAACATCGA GGACGGCAGC GTGCAGCTCG CCGACCACTA CCAGCAGAAC
1501 ACCCCCATCG GCGACGGCCC CGTGCTGCTG CCCGACAACC ACTACCTGAG CTACCAGTCC
1561 GCCCTGAGCA AAGACCCCAA CGAGAAGCGC GATCACATGG TCCTGCTGGA GTTCGTGACC
1621 GCCGCCGGGA TCACTCTCGG CATGGACGAG CTGTACGCAG CCCTGCAGGA GAAGAAGTCA
1681 TGCAGCCAGC GCATGGCCGA ATTCCGGCAA TACTGTTGGA ACCCGGACAC TGGGCAGATG
1741 CTGGGCCGCA CCCCAGCCCG GTGGGTGTGG ATCAGCCTGT ACTATGCAGC TTTCTACGTG
1801 GTCATGACTG GGCTCTTTGC CTTGTGCATC TATGTGCTGA TGCAGACCAT TGATCCCTAC
1861 ACCCCCGACT ACCAGGACCA GTTAAAGTCA CCGGGGGTAA CCTTGAGACC GGATGTGTAT
1921 GGGGAAAGAG GGCTGCAGAT TTCCTACAAC ATCTCTGAAA ACAGCTCTAG ACAGGCCCAG
1981 ATCACCGGAC GTCCGGAGAC TGAGACATTG CCACCGGTAA CGGAATCGGC TGTTGCGCTA
2041 CAGGCGGAGG TGACCCAGAG GGAGCTGTTC GAGTTCGTTC TCAACGACCC CCTCCTCGCC
2101 AGTTCGCTGT ATATTAATAT CGCACTGGCA GGGCTGTCGA TACTGCTTTT CGTGTTCATG
2161 ACGCGCGGAC TCGACGACCC ACGGGCGAAA CTCATCGCCG TTTCGACGAT TTTGGTGCCG
2221 GTGGTCTCTA TCGCGAGCTA CACCGGCCTT GCATCGGGGC TCACCATCAG CGTCCTCGAG
2281 ATGCCAGCCG GCCACTTCGC CGAGGGGTCC TCGGTGATGC TCGGCGGCGA AGAGGTAGAC
2341 GGCGTCGTGA CGATGTGGGG CCGCTATCTG ACGTGGGCCC TTTCGACACC GATGATACTG
2401 CTGGCGCTTG GGCTGCTTGC TGGCTCTAAC GCCACGAAGC TCTTTACCGC CATCACCTTC
2461 GACATCGCGA TGTGTGTCAC CGGCCTCGCA GCCGCGCTGA CGACCTCTTC GCACCTGATG
2521 CGGTGGTTCT GGTACGCCAT CAGTTGTGCG TGTTTCCTCG TCGTCCTCTA CATCCTGCTC
2581 GTCGAGTGGG CACAGGACGC CAAGGCTGCC GGTACTGCGG ATATGTTCAA TACGCTGAAG
2641 CTGCTGACCG TTGTCATGTG GCTCGGCTAC CCCATCGTGT GGGCACTCGG CGTTGAGGGC
2701 ATCGCCGTTC TTCCGGTCGG AGTCACGTCG TGGGGATACA GCTTCCTCGA CATCGTCGCG
2761 AAGTACATCT TCGCGTTCCT GCTGCTCAAC TACCTCACGT CGAACGAGAG CGTCGTCTCC
2821 GGCTCGATAC TCGACGTGCC GTCCGCGTCG GGCACTCCCG CTGACGACTG A
//
```

CONSTRUCT: *hChR2(H134R)-mKate-h(β-bR)* (ACCESSION JN836742)

CDS	*hChR2(H134R)-mKateD-h((HK-β)-bR)*/ 1..2715 bp
hChR2(H134R)	bases 1..927/ amino acids M1--V309/ humanized DNA of protein from ACCESSION AF461397
mKateD	bases 973..1653/ amino acids E7--N233(G166D mutation) of mKate[9,10] from ACCESSION EU383029
rat *hHK-beta*	bases 1657..1962/ amino acids L4--S105/ humanized DNA of protein from ACCESSION M55655
hbR	bases 1966..2712/ amino acids Q1--D249/ humanized DNA of protein from ACCESSION V00474

```
  1 ATGGACTACG GGGGGGCCCT GAGCGCTGTG GGCAGAGAAC TCCTGTTCGT GACAAATCCA
 61 GTCGTGGTGA ACGGCTCCGT ACTCGTACCC GAGGATCAGT GCTATTGCGC AGGATGGATC
121 GAGAGCAGAG GCACAAACGG CGCACAGACT GCATCCAACG TGCTCCAGTG GTTGGCCGCA
181 GGCTTTTCCA TTCTCCTGCT CATGTTTTAC GCCTACCAGA CTTGGAAGTC CACATGTGGC
241 TGGGAGGAAA TCTACGTGTG TGCAATCGAA ATGGTGAAGG TGATCCTGGA GTTTTTCTTC
301 GAATTTAAAA ACCCAAGCAT GCTGTACCTG GCTACTGGCC ACAGAGTGCA GTGGCTGCGG
361 TATGCCGAAT GGCTGCTGAC TTGCCCAGTG ATTCTGATCC GCCTGTCCAA CCTGACTGGG
421 CTGTCTAACG ATTACAGTAG GAGAACAATG GGACTGCTCG TATCCGACAT CGGCACTATC
481 GTATGGGGCG CAACTAGTGC CATGGCCACT GGATACGTGA AAGTGATCTT CTTCTGCCTG
541 GGACTCTGCT ACGGAGCAAA CACATTTTTT CATGCCGCAA AAGCATATAT CGAGGGGTAT
601 CATACCGTCC CAAAGGGCCG GTGTAGACAA GTGGTGACTG GCATGGCTTG GCTGTTCTTC
```

```
 661 GTGTCCTGGG GGATGTTTCC CATCCTCTTT ATCCTGGGCC CAGAAGGCTT CGGGGTGCTG
 721 AGTGTGTATG GCAGTACCGT AGGACACACT ATCATTGACC TGATGAGCAA AAACTGCTGG
 781 GGGCTGCTCG GCCACTACCT GAGAGTACTC ATCCACGAGC ATATCCTGAT TCATGGCGAT
 841 ATCCGGAAAA CTACCAAGCT CAATATCGGG GGCACCGAGA TTGAAGTGGA GACACTCGTG
 901 GAGGACGAGG CCGAGGCCGG AGCAGTGACC GCGGTCGCCA CCATTGTGTC TAAGGGCGAA
 961 GAGCTGATTA AGGAGAACAT GCACATGAAG CTGTACATGG AGGGCACCGT GAACAACCAC
1021 CACTTCAAGT GCACATCCGA GGGCGAAGGC AAGCCCTACG AGGGCACCCA GACCATGAGA
1081 ATCAAGGTGG TCGAGGGCGG CCCTCTCCCC TTCGCCTTCG ACATCCTGGC TACCAGCTTC
1141 ATGTACGGCA GCAAAACCTT CATCAACCAC ACCCAGGGCA TCCCCGACTT CTTTAAGCAG
1201 TCCTTCCCTG AGGGCTTCAC ATGGGAGAGA GTCACCACAT ACGAAGACGG GGGCGTGCTG
1261 ACCGCTACCC AGGACACCAG CCTCCAGGAC GGCTGCCTCA TCTACAACGT CAAGATCAGA
1321 GGGGTGAACT TCCCATCCAA CGGCCCTGTG ATGCAGAAGA AAACACTCGG CTGGGAGGCC
1381 TCCACCGAGA TGCTGTACCC CGCTGACGGC GGCCTGGAAG GCAGAAGCGA CATGGCCCTG
1441 AAGCTCGTGG ACGGGGGCCA CCTGATCTGC AACTTGAAGA CCACATACAG ATCCAAGAAA
1501 CCCGCTAAGA ACCTCAAGAT GCCCGGCGTC TACTATGTGG ACAGAAGACT GGAAAGAATC
1561 AAGGAGGCCG ACAAAGAGAC CTACGTCGAG CAGCACGAGG TGGCTGTGGC CAGATACTGC
1621 GACCTCCCTA GCAAACTGGG GCACAAACTT AATTGCCTGC AGGAGAAGAA ATCCTGTAGC
1681 CAAAGAATGG CCGAATTCAG ACAGTATTGC TGGAATCCCG ATACTGGACA GATGCTGGGG
1741 AGGACACCTG CTAGGTGGGT GTGGATCAGT CTCTATTATG CTGCCTTTTA TGTGGTGATG
1801 ACTGGACTGT TCGCACTGTG CATTTATGTA CTGATGCAGA CCATCGACCC ATATACCCCT
1861 GACTACCAAG ACCAGCTGAA GTCCCCTGGA GTGACACTCA GGCCAGATGT GTACGGCGAG
1921 AGAGGGCTGC AGATCTCCTA CAACATCAGC GAAAATTCCA GCCGGCAAGC CCAGATCACC
1981 GGCCGGCCTG AATGGATCTG GCTCGCACTC GGAACTGCAC TGATGGGGCT CGGGACCCTG
2041 TACTTTCTCG TAAAAGGCAT GGGAGTGTCC GATCCTGATG CCAAAAAGTT CTATGCTATC
2101 ACCACTCTGG TGCCTGCCAT CGCCTTCACC ATGTACCTGT CAATGCTGCT CGGCTACGGC
2161 CTCACAATGG TGCCCTTCGG CGGGGAGCAG AATCCCATCT ACTGGGCAAG ATATGCCGAC
2221 TGGCTGTTTA CAACCCCTCT GCTCCTGCTC GATCTCGCCC TCCTGGTAGA CGCCGATCAA
2281 GGCACTATTC TGGCTTTGGT GGGGGCCGAT GGAATTATGA TTGGGACCGG ACTGGTTGGC
2341 GCCCTGACCA AAGTGTACTC CTACCGGTTC GTGTGGTGGG CCATCTCCAC TGCCGCCATG
2401 CTGTATATCC TCTACGTGCT CTTTTTTGGG TTCACCAGCA AAGCTGAAAG TATGAGGCCT
2461 GAGGTGGCCT CCACATTTAA AGTACTGAGA AACGTGACAG TGGTGCTGTG GAGCGCCTAC
2521 CCTGTGGTGT GGCTGATCGG GTCCGAAGGA GCAGGAATTG TGCCCCTGAA TATTGAAACC
2581 CTGCTGTTCA TGGTCCTGGA CGTGTCCGCA AAGGTAGGGT TCGGACTGAT CCTGCTGCGG
2641 AGTAGGGCAA TTTTTGGCGA GGCTGAGGCC CCAGAGCCTT CCGCCGGGGA TGGCGCAGCC
2701 GCCACCTCCG ACTGA
//
```

CONSTRUCT: *hChR2(C128A)-mKate-h(β-bR)* (ACCESSION JN836743)

CDS	*hChR2(C128A)-mKateAD-h((HK-β)-bR)*/ 1..2715 bp
hChR2(C128A)	bases 1..927/ amino acids M1--V309/ humanized DNA of protein from ACCESSION AF461397
mKateAD	bases 973..1653/ amino acids E7--N233(S158A G166D mutations) of mKate[9,10] from ACCESSION EU383029
rat *hHK-β*	bases 1657..1962/ amino acids L4--S105/ humanized DNA of protein from ACCESSION M55655
hbR	bases 1966..2712/ amino acids Q1--D249/ humanized DNA of protein from ACCESSION V00474

```
   1 ATGGACTACG GGGGGGCCCT GAGCGCTGTG GGCAGAGAAC TCCTGTTCGT GACAAATCCA
  61 GTCGTGGTGA ACGGCTCCGT ACTCGTACCC GAGGATCAGT GCTATTGCGC AGGATGGATC
 121 GAGAGCAGAG GCACAAACGG CGCACAGACT GCATCCAACG TGCTCCAGTG GTTGGCCGCA
 181 GGCTTTTCCA TTCTCCTGCT CATGTTTTAC GCCTACCAGA CTTGGAAGTC CACATGTGGC
 241 TGGGAGGAAA TCTACGTGTG TGCAATCGAA ATGGTGAAGG TGATCCTGGA GTTTTTCTTC
 301 GAATTTAAAA ACCCAAGCAT GCTGTACCTG GCTACTGGCC ACAGAGTGCA GTGGCTGCGG
 361 TATGCCGAAT GGCTGCTGAC TGCCCCAGTG ATTCTGATCC ACCTGTCCAA CCTGACTGGG
 421 CTGTCTAACG ATTACAGTAG GAGAACAATG GGACTGCTCG TATCCGACAT CGGCACTATC
 481 GTATGGGGCG CAACTAGTGC CATGGCCACT GGATACGTGA AAGTGATCTT CTTCTGCCTG
```

```
 541 GGACTCTGCT ACGGAGCAAA CACATTTTTT CATGCCGCAA AAGCATATAT CGAGGGGTAT
 601 CATACCGTCC CAAAGGGCCG GTGTAGACAA GTGGTGACTG GCATGGCTTG GCTGTTCTTC
 661 GTGTCCTGGG GGATGTTTCC CATCCTCTTT ATCCTGGGCC CAGAAGGCTT CGGGGTGCTG
 721 AGTGTGTATG GCAGTACCGT AGGACACACT ATCATTGACC TGATGAGCAA AAACTGCTGG
 781 GGGCTGCTCG GCCACTACCT GAGAGTACTC ATCCACGAGC ATATCCTGAT TCATGGCGAT
 841 ATCCGGAAAA CTACCAAGCT CAATATCGGG GGCACCGAGA TTGAAGTGGA GACACTCGTG
 901 GAGGACGAGG CCGAGGCCGG AGCAGTGACC GCGGTCGCCA CCATTGTGTC TAAGGGCGAA
 961 GAGCTGATTA AGGAGAACAT GCACATGAAG CTGTACATGG AGGGCACCGT GAACAACCAC
1021 CACTTCAAGT GCACATCCGA GGGCGAAGGC AAGCCCTACG AGGGCACCCA GACCATGAGA
1081 ATCAAGGTGG TCGAGGGCGG CCCTCTCCCC TTCGCCTTCG ACATCCTGGC TACCAGCTTC
1141 ATGTACGGCA GCAAAACCTT CATCAACCAC ACCCAGGGCA TCCCCGACTT CTTTAAGCAG
1201 TCCTTCCCTG AGGGCTTCAC ATGGGAGAGA GTCACCACAT ACGAAGACGG GGGCGTGCTG
1261 ACCGCTACCC AGGACACCAG CCTCCAGGAC GGCTGCCTCA TCTACAACGT CAAGATCAGA
1321 GGGGTGAACT TCCCATCCAA CGGCCCTGTG ATGCAGAAGA AAACACTCGG CTGGGAGGCC
1381 TCCACCGAGA TGCTGTACCC CGCTGACGGC GGCCTGGAAG GCAGAGCCGA CATGGCCCTG
1441 AAGCTCGTGG ACGGGGGCCA CCTGATCTGC AACTTGAAGA CCACATACAG ATCCAAGAAA
1501 CCCGCTAAGA ACCTCAAGAT GCCCGGCGTC TACTATGTGG ACAGAAGACT GGAAAGAATC
1561 AAGGAGGCCG ACAAAGAGAC CTACGTCGAG CAGCACGAGG TGGCTGTGGC CAGATACTGC
1621 GACCTCCCTA GCAAACTGGG GCACAAACTT AATTGCCTGC AGGAGAAGAA ATCCTGTAGC
1681 CAAAGAATGG CCGAATTCAG ACAGTATTGC TGGAATCCCG ATACTGGACA GATGCTGGGG
1741 AGGACACCTG CTAGGTGGGT GTGGATCAGT CTCTATTATG CTGCCTTTTA TGTGGTGATG
1801 ACTGGACTGT TCGCACTGTG CATTTATGTA CTGATGCAGA CCATCGACCC ATATACCCCT
1861 GACTACCAAG ACCAGCTGAA GTCCCCTGGA GTGACACTCA GGCCAGATGT GTACGGCGAG
1921 AGAGGGCTGC AGATCTCCTA CAACATCAGC GAAAATTCCA GCCGGCAAGC CCAGATCACC
1981 GGCCGGCCTG AATGGATCTG GCTCGCACTC GGAACTGCAC TGATGGGGCT CGGGACCCTG
2041 TACTTTCTCG TAAAAGGCAT GGGAGTGTCC GATCCTGATG CCAAAAAGTT CTATGCTATC
2101 ACCACTCTGG TGCCTGCCAT CGCCTTCACC ATGTACCTGT CAATGCTGCT CGGCTACGGC
2161 CTCACAATGG TGCCCTTCGG CGGGGAGCAG AATCCCATCT ACTGGGCAAG ATATGCCGAC
2221 TGGCTGTTTA CAACCCCTCT GCTCCTGCTC GATCTCGCCC TCCTGGTAGA CGCCGATCAA
2281 GGCACTATTC TGGCTTTGGT GGGGGCCGAT GGAATTATGA TTGGGACCGG ACTGGTTGGC
2341 GCCCTGACCA AAGTGTACTC CTACCGGTTC GTGTGGTGGG CCATCTCCAC TGCCGCCATG
2401 CTGTATATCC TCTACGTGCT CTTTTTTGGG TTCACCAGCA AAGCTGAAAG TATGAGGCCT
2461 GAGGTGGCCT CCACATTTAA AGTACTGAGA AACGTGACAG TGGTGCTGTG GAGCGCCTAC
2521 CCTGTGGTGT GGCTGATCGG GTCCGAAGGA GCAGGAATTG TGCCCCTGAA TATTGAAACC
2581 CTGCTGTTCA TGGTCCTGGA CGTGTCCGCA AAGGTAGGGT TCGGACTGAT CCTGCTGCGG
2641 AGTAGGGCAA TTTTTGGCGA GGCTGAGGCC CCAGAGCCTT CCGCCGGGGA TGGCGCAGCC
2701 GCCACCTCCG ACTGA
//
```

CONSTRUCT: *hChR2(D156A)-mKate-h(β-bR)* (ACCESSION JN836744)
CDS *hChR2(D156A)-mKateAD-h((HK-β)-bR)*/ 1..2715 bp
hChR2(D156A) bases 1..927/ amino acids M1--V309/ humanized DNA of protein from ACCESSION AF461397
mKateAD bases 973..1653/ amino acids E7--N233(S158A G166D mutation) of mKate[9,10] from ACCESSION EU383029
rat *hHK-β* bases 1657..1962/ amino acids L4--S105/ humanized DNA of protein from ACCESSION M55655
hbR bases 1966..2712/ amino acids Q1--D249/ humanized DNA of protein from ACCESSION V00474

```
   1 ATGGACTACG GGGGGGCCCT GAGCGCTGTG GGCAGAGAAC TCCTGTTCGT GACAAATCCA
  61 GTCGTGGTGA ACGGCTCCGT ACTCGTACCC GAGGATCAGT GCTATTGCGC AGGATGGATC
 121 GAGAGCAGAG GCACAAACGG CGCACAGACT GCATCCAACG TGCTCCAGTG GTTGGCCGCA
 181 GGCTTTTCCA TTCTCCTGCT CATGTTTTAC GCCTACCAGA CTTGGAAGTC CACATGTGGC
 241 TGGGAGGAAA TCTACGTGTG TGCAATCGAA ATGGTGAAGG TGATCCTGGA GTTTTTCTTC
 301 GAATTTAAAA ACCCAAGCAT GCTGTACCTG GCTACTGGCC ACAGAGTGCA GTGGCTGCGG
 361 TATGCCGAAT GGCTGCTGAC TTGCCCAGTG ATTCTGATCC ACCTGTCCAA CCTGACTGGG
```

```
 421 CTGTCTAACG ATTACAGTAG GAGAACAATG GGACTGCTCG TATCCGCCAT CGGCACTATC
 481 GTATGGGGCG CAACTAGTGC CATGGCCACT GGATACGTGA AAGTGATCTT CTTCTGCCTG
 541 GGACTCTGCT ACGGAGCAAA CACATTTTTT CATGCCGCAA AAGCATATAT CGAGGGGTAT
 601 CATACCGTCC CAAAGGGCCG GTGTAGACAA GTGGTGACTG GCATGGCTTG GCTGTTCTTC
 661 GTGTCCTGGG GGATGTTTCC CATCCTCTTT ATCCTGGGCC CAGAAGGCTT CGGGGTGCTG
 721 AGTGTGTATG GCAGTACCGT AGGACACACT ATCATTGACC TGATGAGCAA AAACTGCTGG
 781 GGGCTGCTCG GCCACTACCT GAGAGTACTC ATCCACGAGC ATATCCTGAT TCATGGCGAT
 841 ATCCGGAAAA CTACCAAGCT CAATATCGGG GGCACCGAGA TTGAAGTGGA GACACTCGTG
 901 GAGGACGAGG CCGAGGCCGG AGCAGTGACC GCGGTCGCCA CCATTGTGTC TAAGGGCGAA
 961 GAGCTGATTA AGGAGAACAT GCACATGAAG CTGTACATGG AGGGCACCGT GAACAACCAC
1021 CACTTCAAGT GCACATCCGA GGGCGAAGGC AAGCCCTACG AGGGCACCCA GACCATGAGA
1081 ATCAAGGTGG TCGAGGGCGG CCCTCTCCCC TTCGCCTTCG ACATCCTGGC TACCAGCTTC
1141 ATGTACGGCA GCAAAACCTT CATCAACCAC ACCCAGGGCA TCCCCGACTT CTTTAAGCAG
1201 TCCTTCCCTG AGGGCTTCAC ATGGGAGAGA GTCACCACAT ACGAAGACGG GGGCGTGCTG
1261 ACCGCTACCC AGGACACCAG CCTCCAGGAC GGCTGCCTCA TCTACAACGT CAAGATCAGA
1321 GGGGTGAACT TCCCATCCAA CGGCCCTGTG ATGCAGAAGA AAACACTCGG CTGGGAGGCC
1381 TCCACCGAGA TGCTGTACCC CGCTGACGGC GGCCTGGAAG GCAGAGCCGA CATGGCCCTG
1441 AAGCTCGTGG ACGGGGGCCA CCTGATCTGC AACTTGAAGA CCACATACAG ATCCAAGAAA
1501 CCCGCTAAGA ACCTCAAGAT GCCCGGCGTC TACTATGTGG ACAGAAGACT GGAAAGAATC
1561 AAGGAGGCCG ACAAAGAGAC CTACGTCGAG CAGCACGAGG TGGCTGTGGC CAGATACTGC
1621 GACCTCCCTA GCAAACTGGG GCACAAACTT AATTGCCTGC AGGAGAAGAA ATCCTGTAGC
1681 CAAAGAATGG CCGAATTCAG ACAGTATTGC TGGAATCCCG ATACTGGACA GATGCTGGGG
1741 AGGACACCTG CTAGGTGGGT GTGGATCAGT CTCTATTATG CTGCCTTTTA TGTGGTGATG
1801 ACTGGACTGT TCGCACTGTG CATTTATGTA CTGATGCAGA CCATCGACCC ATATACCCCT
1861 GACTACCAAG ACCAGCTGAA GTCCCCTGGA GTGACACTCA GGCCAGATGT GTACGGCGAG
1921 AGAGGGCTGC AGATCTCCTA CAACATCAGC GAAAATTCCA GCCGGCAAGC CCAGATCACC
1981 GGCCGGCCTG AATGGATCTG GCTCGCACTC GGAACTGCAC TGATGGGGCT CGGGACCCTG
2041 TACTTTCTCG TAAAAGGCAT GGGAGTGTCC GATCCTGATG CCAAAAAGTT CTATGCTATC
2101 ACCACTCTGG TGCCTGCCAT CGCCTTCACC ATGTACCTGT CAATGCTGCT CGGCTACGGC
2161 CTCACAATGG TGCCCTTCGG CGGGGAGCAG AATCCCATCT ACTGGGCAAG ATATGCCGAC
2221 TGGCTGTTTA CAACCCCTCT GCTCCTGCTC GATCTCGCCC TCCTGGTAGA CGCCGATCAA
2281 GGCACTATTC TGGCTTTGGT GGGGGCCGAT GGAATTATGA TTGGGACCGG ACTGGTTGGC
2341 GCCCTGACCA AAGTGTACTC CTACCGGTTC GTGTGGTGGG CCATCTCCAC TGCCGCCATG
2401 CTGTATATCC TCTACGTGCT CTTTTTTGGG TTCACCAGCA AAGCTGAAAG TATGAGGCCT
2461 GAGGTGGCCT CCACATTTAA AGTACTGAGA AACGTGACAG TGGTGCTGTG GAGCGCCTAC
2521 CCTGTGGTGT GGCTGATCGG GTCCGAAGGA GCAGGAATTG TGCCCCTGAA TATTGAAACC
2581 CTGCTGTTCA TGGTCCTGGA CGTGTCCGCA AAGGTAGGGT TCGGACTGAT CCTGCTGCGG
2641 AGTAGGGCAA TTTTTGGCGA GGCTGAGGCC CCAGAGCCTT CCGCCGGGGA TGGCGCAGCC
2701 GCCACCTCCG ACTGA
//
```

CONSTRUCT: *hVChR1-mKate-β-hChR2* (ACCESSION JN836745)

CDS	*hVChR1-mKateA-(HK-β)-hChR2*/ 1..3033 bp
hVChR1	bases 1..900/ amino acids M1--D300/ humanized DNA of protein from ACCESSION EU622855
mKateA	bases 949..1629/ amino acids E7--N233 *mKate(S158A)* from ACCESSION EU383029
rat *HK-β*	bases 1633..1938/ amino acids L4--S105 from ACCESSION V00474
hChR2	bases 1990..2997/ amino acids D2--R337/ humanized DNA of protein from ACCESSION AF461397
PDZ motif	bases 2998..3030/ amino acids C1000—V1010, PDZ binding motif kv1.4 Channel[11,12]

```
  1 ATGGATTACC CTGTGGCCCG GTCCCTGATT GTAAGATACC CCACCGATCT GGGCAATGGA
 61 ACCGTGTGCA TGCCCAGAGG ACAATGCTAC TGCGAGGGGT GGCTGAGGAG CCGGGGCACT
121 AGTATCGAAA AAACCATCGC TATCACCCTC CAGTGGGTAG TGTTCGCTCT GTCCGTAGCC
181 TGTCTCGGCT GGTATGCATA CCAAGCCTGG AGGGCTACCT GTGGGTGGGA GGAAGTATAC
```

```
 241 GTGGCCCTGA TCGAGATGAT GAAGTCCATC ATCGAGGCTT TCCATGAGTT CGACTCCCCA
 301 GCCACACTCT GGCTCAGCAG TGGGAATGGC GTAGTGTGGA TGAGATATGG AGAGTGGCTG
 361 CTGACCTGTC CCGTCCTGCT CATTCATCTG TCCAATCTGA CCGGGCTGAA AGATGACTAC
 421 TCCAAGAGAA CAATGGGACT GCTGGTGAGT GACGTGGGGT GTATTGTGTG GGGAGCCACC
 481 TCCGCCATGT GCACTGGATG GACCAAGATC CTCTTTTTCC TGATTTCCCT CTCCTATGGG
 541 ATGTATACAT ACTTCCACGC CGCTAAGGTG TATATTGAGG CCTTCCACAC TGTACCTAAA
 601 GGCATCTGTA GGGAGCTCGT GCGGGTGATG GCATGGACCT TCTTTGTGGC CTGGGGGATG
 661 TTCCCCGTGC TGTTCCTCCT CGGCACTGAG GGATTTGGCC ACATTAGTCC TTACGGGTCC
 721 GCAATTGGAC ACTCCATCCT GGATCTGATT GCCAAGAATA TGTGGGGGGT GCTGGGAAAT
 781 TATCTGCGGG TAAAGATCCA CGAGCATATC CTGCTGTATG GCGATATCAG AAAGAAGCAG
 841 AAAATCACCA TTGCTGGACA GGAAATGGAG GTGGAGACAC TGGTAGCAGA GGAGGAGGAC
 901 GGGACCGCGG TCGCCACCAT GGTGTCTAAG GGCGAAGAGC TGATTAAGGA GAACATGCAC
 961 ATGAAGCTGT ACATGGAGGG CACCGTGAAC AACCACCACT TCAAGTGCAC ATCCGAGGGC
1021 GAAGGCAAGC CCTACGAGGG CACCCAGACC ATGAGAATCA AGGTGGTCGA GGGCGGCCCT
1081 CTCCCCTTCG CCTTCGACAT CCTGGCTACC AGCTTCATGT ACGGCAGCAA AACCTTCATC
1141 AACCACACCC AGGGCATCCC CGACTTCTTT AAGCAGTCCT TCCCTGAGGG CTTCACATGG
1201 GAGAGAGTCA CCACATACGA AGACGGGGGC GTGCTGACCG CTACCCAGGA CACCAGCCTC
1261 CAGGACGGCT GCCTCATCTA CAACGTCAAG ATCAGAGGGG TGAACTTCCC ATCCAACGGC
1321 CCTGTGATGC AGAAGAAAAC ACTCGGCTGG GAGGCCTCCA CCGAGATGCT GTACCCCGCT
1381 GACGGCGGCC TGGAAGGCAG AGCCGACATG GCCCTGAAGC TCGTGGGCGG GGGCCACCTG
1441 ATCTGCAACT TGAAGACCAC ATACAGATCC AAGAAACCCG CTAAGAACCT CAAGATGCCC
1501 GGCGTCTACT ATGTGGACAG AAGACTGGAA AGAATCAAGG AGGCCGACAA AGAGACCTAC
1561 GTCGAGCAGC ACGAGGTGGC TGTGGCCAGA TACTGCGACC TCCCTAGCAA ACTGGGGCAC
1621 AAACTTAATT GCCTGCAGGA GAAGAAGTCA TGCAGCCAGC GCATGGCCGA ATTCCGGCAA
1681 TACTGTTGGA ACCCGGACAC TGGGCAGATG CTGGGCCGCA CCCCAGCCCG GTGGGTGTGG
1741 ATCAGCCTGT ACTATGCAGC TTTCTACGTG GTCATGACTG GGCTCTTTGC CTTGTGCATC
1801 TATGTGCTGA TGCAGACCAT TGATCCCTAC ACCCCCGACT ACCAGGACCA GTTAAAGTCA
1861 CCGGGGGTAA CCTTGAGACC GGATGTGTAT GGGGAAAGAG GGCTGCAGAT TTCCTACAAC
1921 ATCTCTGAAA ACAGCTCTAG ACAGGCCCAG ATCACCGGAC GTCCGGAGAC TGAGACATTG
1981 CCACCGGTGG ACTACGGGGG GGCCCTGAGC GCTGTGGGCA GAGAACTCCT GTTCGTGACA
2041 AATCCAGTCG TGGTGAACGG CTCCGTACTC GTACCCGAGG ATCAGTGCTA TTGCGCAGGA
2101 TGGATCGAGA GCAGAGGCAC AAACGGCGCA CAGACTGCAT CCAACGTGCT CCAGTGGTTG
2161 GCCGCAGGCT TTTCCATTCT CCTGCTCATG TTTTACGCCT ACCAGACTTG GAAGTCCACA
2221 TGTGGCTGGG AGGAAATCTA CGTGTGTGCA ATCGAAATGG TGAAGGTGAT CCTGGAGTTT
2281 TTCTTCGAAT TTAAAAACCC AAGCATGCTG TACCTGGCTA CTGGCCACAG AGTGCAGTGG
2341 CTGCGGTATG CCGAATGGCT GCTGACTTGC CCAGTGATTC TGATCCACCT GTCCAACCTG
2401 ACTGGGCTGT CTAACGATTA CAGTAGGAGA ACAATGGGAC TGCTCGTATC CGACATCGGC
2461 ACTATCGTAT GGGGCGCAAC TAGTGCCATG GCCACTGGAT ACGTGAAAGT GATCTTCTTC
2521 TGCCTGGGAC TCTGCTACGG AGCAAACACA TTTTTTCATG CCGCAAAAGC ATATATCGAG
2581 GGGTATCATA CCGTCCCAAA GGGCCGGTGT AGACAAGTGG TGACTGGCAT GGCTTGGCTG
2641 TTCTTCGTGT CCTGGGGGAT GTTTCCCATC CTCTTTATCC TGGGCCCAGA AGGCTTCGGG
2701 GTGCTGAGTG TGTATGGCAG TACCGTAGGA CACACTATCA TTGACCTGAT GAGCAAAAAC
2761 TGCTGGGGGC TGCTCGGCCA CTACCTGAGA GTACTCATCC ACGAGCATAT CCTGATTCAT
2821 GGCGATATCC GGAAAACTAC CAAGCTCAAT ATCGGGGGCA CCGAGATTGA AGTGGAGACA
2881 CTCGTGGAGG ACGAGGCCGA GGCCGGAGCA GTGAACAAAG GCACTGGCAA GTATGCCTCC
2941 AGAGAATCCT TTCTGGTGAT GCGGGACAAA ATGAAGGAGA AAGGCATTGA TGTACGGTGC
3001 AGTAATGCCA AAGCCGTCGA GACTGATGTG TAG
//
```

CONSTRUCT: *hVChR1-mKate-β-hChR2(L132C)* (ACCESSION JN836746)

CDS	*hVChR1-mKateA-(HK-β)-hChR2(L132C)*/ 1..3033 bp
hVChR1	bases 1..900/ amino acids M1--D300/ humanized DNA of protein from ACCESSION EU622855
mKateA	bases 949..1629/ amino acids E7--N233 *mKate(S158A)* from ACCESSION EU383029
rat *HK beta*	bases 1633..1938/ amino acids L4--S105 from ACCESSION V00474
hChR2(L132C)	bases 1990..2997/ amino acids D2--R337/ humanized DNA of protein from ACCESSION AF461397

PDZ motif bases 2998..3030/ amino acids C1000—V1010, PDZ binding motif kv1.4 Channel[11,12]

```
   1 ATGGATTACC CTGTGGCCCG GTCCCTGATT GTAAGATACC CCACCGATCT GGGCAATGGA
  61 ACCGTGTGCA TGCCCAGAGG ACAATGCTAC TGCGAGGGGT GGCTGAGGAG CCGGGGCACT
 121 AGTATCGAAA AAACCATCGC TATCACCCTC CAGTGGGTAG TGTTCGCTCT GTCCGTAGCC
 181 TGTCTCGGCT GGTATGCATA CCAAGCCTGG AGGGCTACCT GTGGGTGGGA GGAAGTATAC
 241 GTGGCCCTGA TCGAGATGAT GAAGTCCATC ATCGAGGCTT TCCATGAGTT CGACTCCCCA
 301 GCCACACTCT GGCTCAGCAG TGGGAATGGC GTAGTGTGGA TGAGATATGG AGAGTGGCTG
 361 CTGACCTGTC CCGTCCTGCT CATTCATCTG TCCAATCTGA CCGGGCTGAA AGATGACTAC
 421 TCCAAGAGAA CAATGGGACT GCTGGTGAGT GACGTGGGGT GTATTGTGTG GGGAGCCACC
 481 TCCGCCATGT GCACTGGATG GACCAAGATC CTCTTTTTCC TGATTTCCCT CTCCTATGGG
 541 ATGTATACAT ACTTCCACGC CGCTAAGGTG TATATTGAGG CCTTCCACAC TGTACCTAAA
 601 GGCATCTGTA GGGAGCTCGT GCGGGTGATG GCATGGACCT TCTTTGTGGC CTGGGGGATG
 661 TTCCCCGTGC TGTTCCTCCT CGGCACTGAG GGATTTGGCC ACATTAGTCC TTACGGGTCC
 721 GCAATTGGAC ACTCCATCCT GGATCTGATT GCCAAGAATA TGTGGGGGGT GCTGGGAAAT
 781 TATCTGCGGG TAAAGATCCA CGAGCATATC CTGCTGTATG GCGATATCAG AAAGAAGCAG
 841 AAAATCACCA TTGCTGGACA GGAAATGGAG GTGGAGACAC TGGTAGCAGA GGAGGAGGAC
 901 GGGACCGCGG TCGCCACCAT GGTGTCTAAG GGCGAAGAGC TGATTAAGGA GAACATGCAC
 961 ATGAAGCTGT ACATGGAGGG CACCGTGAAC AACCACCACT TCAAGTGCAC ATCCGAGGGC
1021 GAAGGCAAGC CCTACGAGGG CACCCAGACC ATGAGAATCA AGGTGGTCGA GGGCGGCCCT
1081 CTCCCCTTCG CCTTCGACAT CCTGGCTACC AGCTTCATGT ACGGCAGCAA AACCTTCATC
1141 AACCACACCC AGGGCATCCC CGACTTCTTT AAGCAGTCCT TCCCTGAGGG CTTCACATGG
1201 GAGAGAGTCA CCACATACGA AGACGGGGGC GTGCTGACCG CTACCCAGGA CACCAGCCTC
1261 CAGGACGGCT GCCTCATCTA CAACGTCAAG ATCAGAGGGG TGAACTTCCC ATCCAACGGC
1321 CCTGTGATGC AGAAGAAAAC ACTCGGCTGG GAGGCCTCCA CCGAGATGCT GTACCCCGCT
1381 GACGGCGGCC TGGAAGGCAG AGCCGACATG GCCCTGAAGC TCGTGGGCGG GGGCCACCTG
1441 ATCTGCAACT TGAAGACCAC ATACAGATCC AAGAAACCCG CTAAGAACCT CAAGATGCCC
1501 GGCGTCTACT ATGTGGACAG AAGACTGGAA AGAATCAAGG AGGCCGACAA AGAGACCTAC
1561 GTCGAGCAGC ACGAGGTGGC TGTGGCCAGA TACTGCGACC TCCCTAGCAA ACTGGGGCAC
1621 AAACTTAATT GCCTGCAGGA GAAGAAGTCA TGCAGCCAGC GCATGGCCGA ATTCCGGCAA
1681 TACTGTTGGA ACCCGGACAC TGGGCAGATG CTGGGCCGCA CCCCAGCCCG GTGGGTGTGG
1741 ATCAGCCTGT ACTATGCAGC TTTCTACGTG GTCATGACTG GGCTCTTTGC CTTGTGCATC
1801 TATGTGCTGA TGCAGACCAT TGATCCCTAC ACCCCCGACT ACCAGGACCA GTTAAAGTCA
1861 CCGGGGGTAA CCTTGAGACC GGATGTGTAT GGGGAAAGAG GGCTGCAGAT TTCCTACAAC
1921 ATCTCTGAAA ACAGCTCTAG ACAGGCCCAG ATCACCGGAC GTCCGGAGAC TGAGACATTG
1981 CCACCGGTGG ACTACGGGGG GGCCCTGAGC GCTGTGGGCA GAGAACTCCT GTTCGTGACA
2041 AATCCAGTCG TGGTGAACGG CTCCGTACTC GTACCCGAGG ATCAGTGCTA TTGCGCAGGA
2101 TGGATCGAGA GCAGAGGCAC AAACGGCGCA CAGACTGCAT CCAACGTGCT CCAGTGGTTG
2161 GCCGCAGGCT TTTCCATTCT CCTGCTCATG TTTTACGCCT ACCAGACTTG GAAGTCCACA
2221 TGTGGCTGGG AGGAAATCTA CGTGTGTGCA ATCGAAATGG TGAAGGTGAT CCTGGAGTTT
2281 TTCTTCGAAT TTAAAAACCC AAGCATGCTG TACCTGGCTA CTGGCCACAG AGTGCAGTGG
2341 CTGCGGTATG CCGAATGGCT GCTGACTTGC CCAGTGATTT GCATCCACCT GTCCAACCTG
2401 ACTGGGCTGT CTAACGATTA CAGTAGGAGA ACAATGGGAC TGCTCGTATC CGACATCGGC
2461 ACTATCGTAT GGGGCGCAAC TAGTGCCATG GCCACTGGAT ACGTGAAAGT GATCTTCTTC
2521 TGCCTGGGAC TCTGCTACGG AGCAAACACA TTTTTTCATG CCGCAAAAGC ATATATCGAG
2581 GGGTATCATA CCGTCCCAAA GGGCCGGTGT AGACAAGTGG TGACTGGCAT GGCTTGGCTG
2641 TTCTTCGTGT CCTGGGGGAT GTTTCCCATC CTCTTTATCC TGGGCCCAGA AGGCTTCGGG
2701 GTGCTGAGTG TGTATGGCAG TACCGTAGGA CACACTATCA TTGACCTGAT GAGCAAAAAC
2761 TGCTGGGGGC TGCTCGGCCA CTACCTGAGA GTACTCATCC ACGAGCATAT CCTGATTCAT
2821 GGCGATATCC GGAAAACTAC CAAGCTCAAT ATCGGGGGCA CCGAGATTGA AGTGGAGACA
2881 CTCGTGGAGG ACGAGGCCGA GGCCGGAGCA GTGAACAAAG GCACTGGCAA GTATGCCTCC
2941 AGAGAATCCT TTCTGGTGAT GCGGGACAAA ATGAAGGAGA AAGGCATTGA TGTACGGTGC
3001 AGTAATGCCA AAGCCGTCGA GACTGATGTG TAG
//
```

CONSTRUCT: *ChR2-EYFP-β-Arch* (ACCESSION JN836747)
CDS *ChR2-EYFP-(HK-β)-Arch3*/ 1..2769

ChR2	bases 1..927/ amino acids M1--V309 from ACCESSION AF461397
EYFP	bases 946..1656/ amino acids V2--Y238 from Clontech Data Sheet
rat *HK-β*	bases 1657..1968/ amino acids A2--S105 from ACCESSION M55655
Arch3	bases 1996..2766/ amino acids D2--D258 from ACCESSION GU045593

```
   1 ATGGATTATG GAGGCGCCCT GAGTGCCGTT GGGCGCGAGC TGCTATTTGT AACGAACCCA
  61 GTAGTCGTCA ATGGCTCTGT ACTTGTGCCT GAGGACCAGT GTTACTGCGC GGGCTGGATT
 121 GAGTCGCGTG GCACAAACGG TGCCCAAACG GCGTCGAACG TGCTGCAATG GCTTGCTGCT
 181 GGCTTCTCCA TCCTACTGCT TATGTTTTAC GCCTACCAAA CATGGAAGTC AACCTGCGGC
 241 TGGGAGGAGA TCTATGTGTG CGCTATCGAG ATGGTCAAGG TGATTCTCGA GTTCTTCTTC
 301 GAGTTTAAGA ACCCGTCCAT GCTGTATCTA GCCACAGGCC ACCGCGTCCA GTGGTTGCGT
 361 TACGCCGAGT GGCTTCTCAC CTGCCCGGTC ATTCTCATTC ACCTGTCAAA CCTGACGGGC
 421 TTGTCCAACG ACTACAGCAG GCGCACCATG GGTCTGCTTG TGTCTGATAT TGGCACAATT
 481 GTGTGGGGCG CCACTTCCGC CATGGCCACC GGATACGTCA AGGTCATCTT CTTCTGCCTG
 541 GGTCTGTGTT ATGGTGCTAA CACGTTCTTT CACGCTGCCA AGGCCTACAT CGAGGGTTAC
 601 CACACCGTGC CGAAGGGCCG GTGTCGCCAG GTGGTGACTG GCATGGCTTG GCTCTTCTTC
 661 GTATCATGGG GTATGTTCCC CATCCTGTTC ATCCTCGGCC CCGAGGGCTT CGGCGTCCTG
 721 AGCGTGTACG GCTCCACCGT CGGCCACACC ATCATTGACC TGATGTCGAA GAACTGCTGG
 781 GGTCTGCTCG GCCACTACCT GCGCGTGCTG ATCCACGAGC ATATCCTCAT CCACGGCGAC
 841 ATTCGCAAGA CCACCAAATT GAACATTGGT GGCACTGAGA TTGAGGTCGA GACGCTGGTG
 901 GAGGACGAGG CCGAGGCTGG CGCGGTACCC GCGGCCGCCA CCATTGTGAG CAAGGGCGAG
 961 GAGCTGTTCA CCGGGGTGGT GCCCATCCTG GTCGAGCTGG ACGGCGACGT AAACGGCCAC
1021 AAGTTCAGCG TGTCCGGCGA GGGCGAGGGC GATGCCACCT ACGGCAAGCT GACCCTGAAG
1081 TTCATCTGCA CCACCGGCAA GCTGCCCGTG CCCTGGCCCA CCCTCGTGAC CACCTTCGGC
1141 TACGGCCTGC AGTGCTTCGC CCGCTACCCC GACCACATGA AGCAGCACGA CTTCTTCAAG
1201 TCCGCCATGC CCGAAGGCTA CGTCCAGGAG CGCACCATCT TCTTCAAGGA CGACGGCAAC
1261 TACAAGACCC GCGCCGAGGT GAAGTTCGAG GGCGACACCC TGGTGAACCG CATCGAGCTG
1321 AAGGGCATCG ACTTCAAGGA GGACGGCAAC ATCCTGGGGC ACAAGCTGGA GTACAACTAC
1381 AACAGCCACA ACGTCTATAT CATGGCCGAC AAGCAGAAGA ACGGCATCAA GGTGAACTTC
1441 AAGATCCGCC ACAACATCGA GGACGGCAGC GTGCAGCTCG CCGACCACTA CCAGCAGAAC
1501 ACCCCCATCG GCGACGGCCC CGTGCTGCTG CCCGACAACC ACTACCTGAG CTACCAGTCC
1561 GCCCTGAGCA AAGACCCCAA CGAGAAGCGC GATCACATGG TCCTGCTGGA GTTCGTGACC
1621 GCCGCCGGGA TCACTCTCGG CATGGACGAG CTGTACGCAG CCCTGCAGGA GAAGAAGTCA
1681 TGCAGCCAGC GCATGGCCGA ATTCCGGCAA TACTGTTGGA ACCCGGACAC TGGGCAGATG
1741 CTGGGCCGCA CCCCAGCCCG GTGGGTGTGG ATCAGCCTGT ACTATGCAGC TTTCTACGTG
1801 GTCATGACTG GGCTCTTTGC CTTGTGCATC TATGTGCTGA TGCAGACCAT TGATCCCTAC
1861 ACCCCCGACT ACCAGGACCA GTTAAAGTCA CCGGGGGTAA CCTTGAGACC GGATGTGTAT
1921 GGGGAAAGAG GGCTGCAGAT TTCCTACAAC ATCTCTGAAA ACAGCTCTAG ACAGGCCCAG
1981 ATCACCGGAC GTCCGGACCC CATCGCTCTG CAGGCTGGTT ACGACCTGCT GGGTGACGGC
2041 AGACCTGAAA CTCTGTGGCT GGGCATCGGC ACTCTGCTGA TGCTGATTGG AACCTTCTAC
2101 TTTCTGGTCC GCGGATGGGG AGTCACCGAT AAGGATGCCC GGGAATATTA CGCTGTGACT
2161 ATCCTGGTGC CCGGAATCGC ATCCGCCGCA TATCTGTCTA TGTTCTTTGG TATCGGGCTT
2221 ACTGAGGTGA CCGTCGGGGG CGAAATGTTG GATATCTATT ATGCCAGGTA CGCCGACTGG
2281 CTGTTTACCA CCCCACTTCT GCTGCTGGAT CTGGCCCTTC TCGCTAAGGT GGATCGGGTG
2341 ACCATCGGCA CCCTGGTGGG TGTGGACGCC CTGATGATCG TCACTGGCCT CATCGGAGCC
2401 TTGAGCCACA CGGCCATAGC CAGATACAGT TGGTGGTTGT TCTCTACAAT TTGCATGATA
2461 GTGGTGCTCT ATTTTCTGGC TACATCCCTG CGATCTGCTG CAAAGGAGCG GGGCCCCGAG
2521 GTGGCATCTA CCTTTAACAC CCTGACAGCT CTGGTCTTGG TGCTGTGGAC CGCTTACCCT
2581 ATCCTGTGGA TCATAGGCAC TGAGGGCGCT GGCGTGGTGG GCCTGGGCAT CGAAACTCTG
2641 CTGTTTATGG TGTTGGACGT GACTGCCAAG GTCGGCTTTG GCTTTATCCT GTTGAGATCC
2701 CGGGCTATTC TGGGCGACAC CGAGGCACCA GAACCCAGTG CCGGTGCCGA TGTCAGTGCC
2761 GCCGACTAA
```

Supplementary Note 5

Consideration of the ChR2 desensitization for pump ion-turnover calculations

Initially considering the ChR2 steady-state currents lead to pump turnovers that were systematically higher than expected from the measured pump relaxation times (**Table 1**). However, when the ChR2 peak currents were considered, the determined turnovers agreed with the expected values. This is a result of the ChR2 desensitization, reflected in the transition from the peak to the steady-state current, which is equivalent to a reduction of active ChR2 molecules. While consideration of the ChR2 desensitization is important for the determination of absolute pump turnover numbers, a comparison of relative pump turnovers is not affected by referencing to either ChR2 steady-state or peak current. The ChR2 steady state-to-peak current ratios after full dark-adaptation measured in HEK293 cells under the given ionic and saturating light conditions as well as optimal time resolution were 0.37 ± 0.07 (mean ± s.e.m.) for the wild-type[13], 0.52 ± 0.04 (n=5, mean ± s.e.m.) for ChR2(H134R) and 0.60 ± 0.20 (mean ± s.e.m.) for CatCh[13]. Thus, the ChR2 peak current densities for pump ion-turnover calculations were reconstructed from the measured stationary ChR2 current densities (**Table 1**) multiplied by the desensitization correction factor f_D (multiplicative inverse of the steady state-to-peak current ratios), which is 2.7 for ChR2 and 1.9 for hChR2(H134R).

References

1. Thyagarajan, S. *et al.* Visual function in mice with photoreceptor degeneration and transgenic expression of channelrhodopsin 2 in ganglion cells. *J Neurosci* **30**, 8745-8758 (2010).
2. Bamberg, E., Tittor, J. & Oesterhelt, D. Ligt-driven proton or chloride pumping by halorhodopsin. *Proc Natl Acad Sci USA* **90**, 639-643 (1993).
3. Chizhov, I. & Engelhard, M. Temperature and halide dependence of the photocycle of halorhodopsin from *Natronobacterium pharaonis*. *Biophys J* **81**, 1600-1612 (2001).
4. Chizhov, I. *et al.* Spectrally silent transitions in the bacteriorhodopsin photocycle. *Biophys J* **71**, 2329-2345 (1996).
5. Váró, G. *et al.* Light-driven chloride ion transport by halorhodopsin from *Natronobacterium pharaonis*. I. The photochemical cycle. *Biochemistry* **34**, 14490-14499 (1995).
6. Geibel, S. *et al.* The voltage-dependent proton pumping in bacteriorhodopsin is characterized by optoelectic behavior. *Biophys J* **81**, 2059-2068 (2001).
7. Seki, A. *et al.* Heterologous expression of Pharaonis halorhodopsin in *Xenopus laevis* oocytes and electrophysiological characterization of its light-driven Cl^- pump activity. *Biophys J* **92**, 2559-2569 (2007).
8. Zhang, F. *et al.* Multimodal fast optical interrogation of neural circuitry. *Nature* **446**, 633-639 (2007).
9. Pletnev, S. *et al.* A crystallographic study of bright far-red fluorescent protein mKate reveals pH-induced cis-trans isomerization of the chromophore. *J Biol Chem* **283**, 28980–28987 (2008).

10. Shcherbo, D. *et al.* Bright far-red fluorescent protein for whole-body imaging. *Nat Methods* **4**, 741-746 (2007).
11. Lim, I., Hall, D., Hell, J. & . . Selectivity and promiscuity of the first and second PDZ domains of PSD-95 and synapse-associated protein 102. *J Biol Chem* **277**, 21697-21711 (2002).
12. Wong, W. & Schlichter, L. Differential recruitment of Kv1.4 and Kv4.2 to lipid rafts by PSD-95. *J Biol Chem* **279**, 444-452 (2004).
13. Kleinlogel, S. *et al.* Ultra light-sensitive and fast neuronal activation with the $Ca2^{+}$-permeable channelrhodopsin CatCh. *Nat Neurosci* **14**, 513-518 (2011).